Zoological Journal of the Linnean Society, 2006, **148**, 133–168. With 14 figures

Bone surface texture as an ontogenetic indicator in long bones of the Canada goose *Branta canadensis* (Anseriformes: Anatidae)

ALLISON R. TUMARKIN-DERATZIAN[1]*, DAVID R. VANN[2] and PETER DODSON[2,3]

[1]*Department of Geology and Geography, Vassar College, Poughkeepsie, New York, USA*
[2]*Department of Earth and Environmental Science, University of Pennsylvania, Philadelphia, Pennsylvania, USA*
[3]*Department of Animal Biology, University of Pennsylvania School of Veterinary Medicine, Philadelphia, Pennsylvania, USA*

Received February 2005; accepted for publication October 2005

Growth series of femora, tibiotarsi, and humeri of the Canada goose *Branta canadensis* were examined to evaluate whether bone surface textures are reliable indicators of relative age and skeletal maturity in this taxon. The relationship between surface texture and skeletal maturity was analysed by comparing element texture types with both size-based and size-independent maturity estimates. A subsample of hindlimb elements was thin sectioned to observe histological structures underlying various surface textures. Three relative age classes of elements are identifiable based on surface texture. Juvenile and subadult bone textures have fibrous and/or porous areas on the bone shaft and are distinguished by the presence (in juveniles) or absence (in subadults) of coarse longitudinal striations in proximal and/or distal regions. Adult bone texture lacks surface porosity. Immature textures are caused by channels in fibrolamellar bone intersecting the bone surface; the presence or absence of striations is determined by channel orientation. Mature textures may be underlain by fibrolamellar bone with little to no surface exposure of channels, or by lamellar bone deposited after rapid growth ceases. The utility of the textural ageing method appears intimately related to the uninterrupted determinate growth regime of *Branta*. This suggests that bone surface textures may prove useful as skeletal maturity indicators in both modern and fossil taxa with similar growth regimes, but may not necessarily be reliable for taxa with interrupted and/or indeterminate growth.

ADDITIONAL KEYWORDS: bird – growth – histology – maturity – skeleton.

INTRODUCTION

The assessment of ontogenetic status from skeletal material is an essential issue in vertebrate palaeontology and archaeozoology. The reliable differentiation of juvenile, subadult, and adult representatives of given taxa is crucial for addressing taxonomic, phylogenetic, and ecological questions. Additionally, the age structure of animal remains in archaeological sites can be an important tool for interpreting seasonality of site occupation and economic uses of domestic species. Body or skeletal element size ideally should not be used as the sole criterion for recognizing age classes, as individual growth variations may make small adults nearly indistinguishable from large juveniles or subadults. Size-independent criteria widely used for evaluating ontogenetic stages in skeletal material include ossification of limb bone ends (e.g. Benecke, 1993; Bennett, 1993; Cohen & Serjeantson, 1996; Gotfredsen, 1997; Serjeantson, 1998, 2002; Mannermaa, 2002), fusion of epiphyses and compound skeletal elements (e.g. Carey, 1982; Sadler, 1991; Brochu, 1996; Cohen & Serjeantson, 1996; Gotfredsen, 1997; Serjeantson, 1998, 2002; Gotfredsen, 2002), and relative development of secondary sexual characteristics such as cranial display structures (e.g. Dodson, 1975; Sampson, Ryan & Tanke, 1997). Such methods require the preservation of the relevant skeletal elements, making them less useful for ageing incomplete,

*Corresponding author. Current address: Department of Geology, Temple University, Philadelphia, Pennsylvania, USA. E-mail: altd@temple.edu

fragmentary, or disarticulated specimens. A potential method for assessing relative age from isolated remains relies on a distinction between immature and mature textures on bone surfaces. In this context, the terms 'immature' and 'mature' designate only stages in the development and growth of the skeleton (*sensu* Bennett, 1993; Brochu, 1996; Serjeantson, 1998), and do not imply any assumptions of sexual development or reproductive status.

Texture-based estimates of relative skeletal maturity have been applied to a variety of fossil vertebrates. Johnson (1977) reported textural differences in ichthyosaur humeri, noting a rough porous texture on immature bones in contrast to a smooth surface on mature elements. Callison & Quimby (1984) and Brinkman (1988) distinguished juveniles and subadults from adults among small theropod dinosaurs and pelycosaurs, respectively, based on the relative ossification of limb bone surfaces. Jacobs *et al*. (1994) and Brill & Carpenter (2001) noted spongy and fibrous textures on juvenile ankylosaur and ornithopod bone. Bennett (1993) examined ontogeny in the long bones of pterodactyloid pterosaurs, and characterized subadult bone as having a porous texture absent in adult elements. Sampson *et al*. (1997) and Ryan *et al*. (2001) described three textural age classes in skulls of the horned dinosaurs *Centrosaurus*, *Einiosaurus*, and *Pachyrhinosaurus*: a juvenile texture characterized by parallel striations generally orientated in the direction of growth, an adult texture characterized by the absence of the juvenile type (but varying from smooth to rugose depending on the individual and anatomical area in question), and an intermediate subadult texture comprising a mottled mosaic of striated and nonstriated regions. Carr (1999) applied the textural classes of Bennett (1993) and Sampson *et al*. (1997) to an analysis of ontogeny in tyrannosaurid theropods. Sampson *et al*. (1997) proposed the name 'periosteal ageing' for this method, as it is based on observations of the external surface of the bone, which would have been covered in life by the periosteum. This term has the potential to be misleading outside of palaeontological circles, in that it may imply ageing based on features of the periosteum itself in cases where soft tissue is present. A less confusing term in this context may be simply 'textural ageing'.

Detailed examinations of the relationship between bone surface texture and skeletal maturity in extant taxa are conspicuously lacking, although generalized differences in textures of immature and mature bone similar to those described in the fossil record have been noted for modern reptiles and birds. Johnson (1977) hypothesized that removal of the periosteum from the actively growing bone of young crocodylians would reveal a pitted surface texture, whereas a smooth surface would be expected in older animals in which appositional growth had slowed, but did not cite actual observations of crocodylian bone. The degree of ossification and the general presence or absence of porosity have been used to separate immature from mature birds in archaeozoological samples (Benecke, 1993; Cohen & Serjeantson, 1996; Gotfredsen, 1997; Serjeantson, 1998, 2002; Mannermaa, 2002). Most authors recognize only two age classes (immature and mature, or juvenile and adult). However, Gotfredsen (1997) combined observations of porosity with the degree of epiphyseal fusion to distinguish juveniles, subadults, and adults. Callison & Quimby (1984) examined femora, tibiotarsi, and tarsometatarsi of immature and mature *Struthio*, *Pterocnemia*, *Rhea*, *Casuarius*, *Meleagris*, and *Gallus*, concluding that immature bones may be distinguished by the presence of longitudinally orientated lineations as well as surface exposure of spongy bone. They noted that textures become progressively fainter and disappear as the birds mature, and reported the occurrence of the immature texture in individuals up to 75% full adult size. The persistence of porous immature textures on bones at or near adult size has also been noted in *Grus* (Serjeantson, 1998), *Cepphus* (Mannermaa, 2002), and *Anser* (Serjeantson, 2002). Sanz *et al*. (1997) noted clusters of tiny foramina on the mandible, cervical vertebrae, and long bone shafts of a Cretaceous bird nestling, and compared these with similar patterns of grooves and pores caused by incomplete ossification of periosteal bone in extant neonate birds. They noted that in modern taxa, surface grooves gradually diminish in prominence and are first converted to isolated foramina before disappearing during the first few weeks posthatching. In larger-bodied species, surface features tend to persist longer than in smaller-bodied taxa (Sanz *et al*., 1997). This may reflect differences in the growth pattern between smaller and larger species, as a longer period of slow, residual growth before reaching adult size has been suggested for small-bodied taxa (Ponton *et al*., 2004).

Rapid bone growth has been hypothesized as the cause of the immature textures, with mature textures attributed to a cessation or dramatic slowing of osteogenesis during the ageing process (Johnson, 1977; Bennett, 1993; Sampson *et al*., 1997; Ryan *et al*., 2001). Studies of pterodactyloid pterosaur bone histology (Bennett, 1993; de Ricqlès, Padian & Horner, 1993; de Ricqlès *et al*., 2000; Sayão, 2003) seem to support a link between surface textures and ossification and vascularization patterns. Several histological studies of long bone ontogeny in dinosaurs and fossil birds [Chinsamy (1990, 1993, 1995b) for *Syntarsus*, *Massospondylus*, and *Dryosaurus*; Varricchio (1993) for *Troodon*; Horner & Currie (1994) for *Hypacrosaurus*; Curry (1999) for *Apatosaurus*; Horner, de Ricqlès & Padian (1999, 2000) for *Hypacrosaurus* and *Maia-*

saura; Sander (2000) for *Barosaurus*, *Brachiosaurus*, *Dicraeosaurus*, and *Janenschia*; Chinsamy & Elzanowski (2001) for *Gobipteryx*; de Ricqlès *et al*. (2003) for *Confuciusornis*; and Padian, Horner & de Ricqlès (2004) for *Orodromeus* and *Confuciusornis*] reveal decreasing vascularization in the outer bony cortex with increasing age. These ontogenetic changes suggest correlative textural changes at the macroscopic level. In most of these studies, the authors did not directly address the issue of surface texture, although Horner & Currie (1994) did associate a rough highly porous texture on embryonic and nestling *Hypacrosaurus* long bones with a fibrolamellar cortex and extensive penetrations of the bone surface by vascular canals.

The use of bone surface texture as an ontogenetic indicator theoretically has the potential to be broadly applicable across skeletal elements and across taxa. However, such possibilities have yet to be rigorously tested in either fossil or modern animals. There is at present a critical need for a detailed investigation of bone surface textures in extant vertebrates, in order to identify specific textural changes within taxa, to evaluate whether universal patterns of textural change are likely to exist, and to determine the underlying biological causes of different textural types. This study begins such testing through the macroscopic and histological evaluation of ontogenetic bone texture changes in the Canada goose *Branta canadensis* Linnaeus.

Several concerns influenced the choice of *B. canadensis* as a study taxon. Previous discussions of ontogenetic bone texture change have largely focused on members of the Archosauria, specifically dinosaurs, pterosaurs, and birds. Following this lead, it is appropriate for a detailed study of modern taxa to begin with the extant archosaurs, birds and crocodylians. [Tumarkin-Deratzian (2002) reported preliminary results from a companion study on textural ageing in the American alligator *Alligator mississippiensis*.] *B. canadensis* was primarily chosen due to its abundance and the consequent availability of a large study sample representing a wide age range of wild individuals. A large-bodied taxon was also desirable for a detailed macroscopic textural analysis, as the reliable documentation of texture types and distributions is facilitated on larger elements where textures are more readily visible. With the exception that males are slightly heavier than females (Johnsgard, 1975; Palmer & MacInnes in Palmer, 1976), *B. canadensis* is sexually monomorphic (Johnson & Castelli, 1998), thus reducing the likelihood that sexually dimorphic variation will seriously interfere with observations of ontogenetic effects. Anseriformes are among the most basal of modern neognathous birds (Cracraft, 1986); this has implications for comparing the results of this study with those focusing on other archosaurs. Finally, geese (*Anser* and *Branta*) are common components of archaeozoological assemblages, as both wild and domestic species. Given the practice of using flock age structures as a means for inferring economic uses of domestic birds (e.g. Benecke, 1993; Hutton MacDonald, MacDonald & Ryan, 1993; Serjeantson, 2002), the establishment of a detailed and reliable textural ageing method for goose bones would be of great utility for zooarchaeological studies.

Institutional abbreviations

DMNH, Delaware Museum of Natural History, Wilmington, Delaware; TSBR, Tri-State Bird Rescue and Research, Newark, Delaware.

MATERIAL AND METHODS

The skeletons of 73 *B. canadensis* individuals in the DMNH osteology collection were examined. Eight additional individuals were obtained directly from TSBR. The femur, tibiotarsus, and humerus were examined for each individual as available. Preference was given to right-side elements; left-side bones were used in cases where right-side elements were missing, broken, pathological, or too greasy to permit reliable textural observations.

The majority of *B. canadensis* skeletons in the DMNH collection represent individuals obtained initially from TSBR, along with medical treatment records, following natural death or euthanasia due to a poor prognosis. Dates of death were known for all but one individual (DMNH 82688). Associated sex and age data were also available for most of the birds, although age data were only in general terms such as 'gosling', 'immature', 'adult', etc. Birds in the DMNH collection represent multiple populations from several north-east and mid-Atlantic states (Table 1). Both resident and migrant flocks exist in these study sample source areas. Resident flocks breed locally and reside essentially year-round (Palmer, 1976; Sheaffer & Malecki, 1998; Hess *et al*., 2000); migrant flocks breed in sub-Arctic Canada and winter in the study sample source regions beginning in October to December through to February or March. Peak departure and arrival dates vary somewhat north to south, with earlier arrivals and later departures in northern localities (Bellrose, 1980; Meanley, 1982; Hartman & Dunn, 1998; Hess *et al*., 2000). The probable mix of residents and migrants within the DMNH collection has important implications for the taxonomic composition of the study sample.

The species *B. canadensis* has been variously separated into eight to 12 subspecies or races (Table 2) based on geographical range, body size, and plumage

characters (Delacour, 1951, 1954; Palmer, 1976; Bellrose, 1980). Determining the subspecific make-up of any given geographical region is confounded by several factors, including questionable divisions among subspecies, the multirace nature of wintering migrant flocks, and the release of captive flocks and the establishment of new feral resident populations outside the presumed original range of certain subspecies (Delacour, 1951, 1954; Palmer, 1976; Hess *et al*., 2000).

Table 1. Source localities of study sample individuals

State	County	Number of individuals
Delaware		47
	Kent	1
	New Castle	40
	Sussex	6
Maryland		6
	Caroline	1
	Cecil	3
	Kent	1
	Worcester	1
New Jersey		2
	Gloucester	2
New York		2
	Ulster	2
Pennsylvania		21
	Chester	15
	Delaware	3
	Montgomery	2
	Philadelphia	1
Virginia		3
	Fairfax	3

Migrant flocks that winter in the study sample source areas are combinations of individuals from the North Atlantic and mid-Atlantic breeding populations (Bellrose, 1980; Owen, 1980; Hess *et al*., 2000). The North Atlantic population comprises the subspecies *B. c. canadensis*, which breeds east of 70° west longitude in Labrador, Quebec, and Newfoundland. The mid-Atlantic population breeds between 70 and 95° west longitude in the Hudson Bay lowlands of Ontario and Quebec, and is composed of *B. c. interior*. Migrant individuals in the study sample may therefore include representatives of *B. c. canadensis* and/or *B. c. interior* (Delacour, 1954; Johnsgard, 1975; Bellrose, 1980; Owen, 1980; Stotts, 1983).

Resident populations were probably established from stocks of *B. c. maxima* and *B. c. moffitti* introduced by the liberation of captive flocks and subsequent restocking (Palmer, 1976; Stotts, 1983; Nelson & Oetting, 1998; Hess *et al*., 2000). Palmer (1976) and Owen (1980) contended that these subspecies should be collapsed into a single subspecies *B. c. moffitti*. Stotts (1983) noted that, although the resident flocks are primarily *B. c. moffitti* (*B. c. maxima*), some resident *B. c. interior* and/or *B. c. canadensis* may be present as well. Palmer (1976) also noted the presence of resident flocks of *B. c. interior*, again presumably descendants of introduced or restocked birds. One must assume, therefore, that the DMNH/TSBR study sample may include individuals representing three or four separate subspecies (*B. c. canadensis*, *B. c. interior*, *B. c. maxima*, *B. c. moffitti*), depending on whether *B. c. maxima* is considered distinct from *B. c. moffitti*.

The sizes of adult *B. canadensis* vary widely by subspecies, with body weights ranging from 0.9 kg in female *B. c. minima* to 5.4 kg in large male

Table 2. Overview of the subspecific taxonomy of *Branta canadensis*

Delacour (1954)		Palmer (1976)		Bellrose (1980)	
Subspecies	Race name	Subspecies	Race name	Subspecies	Race name
B. c. canadensis	Atlantic	*B. c. canadensis*	Atlantic	*B. c. canadensis*	Atlantic
B. c. interior	Interior	*B. c. interior*	Interior	*B. c. interior*	Interior
B. c. moffitti	Moffitt's	*B. c. moffitti* (includes *B. c. maxima*)	Giant	*B. c. moffitti*	Western
B. c. maxima	Giant			*B. c. maxima*	Giant
B. c. parvipes	Lesser	*B. c. parvipes* (includes *B. c. taverneri*)	Lesser	*B. c. parvipes*	Lesser
B. c. taverneri	Taverner's			*B. c. taverneri*	Taverner's
B. c. occidentalis	Dusky	*B. c. occidentalis* (includes *B. c. fulva*)	Dusky	*B. c. occidentalis*	Dusky
B. c. fulva	Vancouver			*B. c. fulva*	Vancouver
B. c. leucopareia	Aleutian	*B. c. leucopareia* (includes *B. c. asiatica*)	Aleutian	*B. c. leucopareia*	Aleutian
B. c. asiatica	Bering				
B. c. minima	Cackling	*B. c. minima*	Cackling	*B. c. minima*	Cackling
B. c. hutchinsi	Richardson's	*B. c. hutchinsii*	Richardson's	*B. c. hutchinsii*	Richardson's

B. c. maxima (Delacour, 1954; Palmer, 1976; Bellrose, 1980; Meanley, 1982). The largest subspecies are *B. c. maxima* and *B. c. moffitti*, averaging 3.7 kg in adult females and 4.5 kg in adult males. *B. c. interior* and *B. c. canadensis* are slightly smaller, with adult females averaging 3.8 and 3.3 kg and adult males 4.2 and 3.8 kg, respectively (Johnsgard, 1975). The weight of newly hatched *B. canadensis* goslings averages approximately 103 g (Elder in Palmer, 1976). Gosling growth rates vary depending on the quality and quantity of available food resources (Leafloor, Ankney & Rusch, 1998; Cooch, Dzubin & Rockwell, 1999), but the skeleton generally reaches adult size by the time of fledging (Owen, 1980), which occurs 8–9 weeks post-hatching in the larger subspecies (Elder in Palmer, 1976). Adult weights, however, may not be attained until after the second winter of life; this results from differences in muscle mass in younger and older birds (Hanson, 1965, 1967).

Among the larger subspecies, successful breeding occurs in approximately one-third of 2 year olds and all breed by age 3 years [data for *B. c. moffitti* from Craighead & Stockstad (1964)]. Breeding and nesting times are influenced by temperature and weather conditions; there is, therefore, geographical variation as well as potential yearly variation due to early or late arrival of the spring season (Elder in Palmer, 1976). Among resident populations within source areas for study birds, clutch completion dates generally peak in early to mid-April (Hess *et al*., 2000). The clutch size averages five eggs, and the incubation period averages 28 days (Delacour, 1954). Goslings hatch in early to mid-May, and fledging occurs in July.

Estimating skeletal maturity

For the purposes of this study, maturity refers to full development of the skeleton when applied to individuals, and of the element in question when applied to bones themselves. Maturity in this context is not meant to imply correlation with sexual or reproductive maturity as relates to breeding age. Skeletal maturity occurs by the end of the first calendar year of life, at approximately 7 months of age. In contrast, most birds do not breed successfully until aged 2 or 3 years (Craighead & Stockstad, 1964).

Separate maturity estimates were performed for the femur, tibiotarsus, and humerus, and three independent estimates (one size-based, two size-independent) were used within each growth series. The size-based estimate was element length as a percentage of average adult length for the species. Lengths were measured following the conventions of Gilbert, Martin & Savage (1996). For the femur, measured length is the distance from the most proximal point on the greater trochanter to the most distal point on the lateral condyle; for the tibiotarsus, from the most proximal point on the cranial cnemial crest to the most distal point on the lateral condyle; and for the humerus, from the most proximal point on the humeral head to the most distal point on the medial condyle. Lengths of immature bones with unossified ends were measured from the most proximal to the most distal point. Three replicates of each measurement were made with digital callipers; the values reported here are means of the replicates. The standards used to calculate the percentage of adult size were mean values computed from the minimum and maximum adult sizes reported by Gilbert *et al*. (1996) (Table 3). In many cases, element lengths in the present sample exceeded this average, resulting in percentages of up to 120% adult size. This probably reflects the small sample measured by Gilbert *et al*. (1996) and the large size range occupied by the various subspecies of *B. canadensis*. Given that the resident portion of the study sample was probably mostly composed of individuals from the largest subspecies (*B. c. maxima* and/or *B. c. moffitti*), it is not unexpected that adult size values will be slightly higher than a mean value for the species as a whole.

For the size-independent maturity estimates, character matrices were constructed for each element based on presence/absence data for muscle scars and other bony landmarks visible in the largest and thus presumably oldest animals. Characters and character states for each element are listed in Appendix 1. A feature was considered present if it was visible under a 10× hand lens. Bone landmark data were analysed by two separate methods.

The first method was derived from a parsimony-based technique used by Brochu (1996) to assess relative skeletal maturity in the American alligator. Redundant individuals (those with the exact same suite of character states) were omitted from this analysis to reduce the volume in the data set (Appendix 2). The outgroup was coded as a form lacking all bony landmarks considered. The resulting data matrix was analysed using the branch-and-bound algorithm of PAUP, version 4.0b10 (Swofford, 1999). Analyses yielded multiple most-parsimonious trees for each of the three elements examined; strict consensus trees

Table 3. Range of long bone lengths (mm) for *Branta canadensis*, as reported by Gilbert *et al*. (1996)

Element	Minimum length	Maximum length	Mean	*N*
Femur	77	86	81.5	7
Tibiotarsus	141	160	150.5	7
Humerus	164	181	172.5	7

were generated to identify common nodes. Nodes on consensus trees were treated as discrete ontogenetic stages in the development of the element in question. Stages were therefore defined by the characters defining the consensus nodes, except those characters that reversed higher up the tree or arose independently at more than one nonconsecutive node; these were treated as unreliable indicators and not included in stage definitions. Once ontogenetic stages were recognized, the percentage maturity of each bone was expressed mathematically as a percentage of the total number of stages through which that element must pass before attaining full maturity. Thus, a bone at stage 2 out of four total stages received a percentage maturity value of 50%.

A potential flaw in the parsimony-based method arises from the fact that PAUP is optimized for the construction of phylogenetic cladograms. Although it can be argued that the accumulation of characters during ontogeny is not totally dissimilar to the evolutionary appearance of characters in a clade, PAUP is ill-equipped to deal with the ambiguities that arise if characters do not always arise in a linear sequential series of events. The bone landmark data were therefore also analysed by a second method, in which hierarchical clustering analysis was used to test for natural groups of specimens with similar characters. A normalized percent disagreement metric was used as the distance metric; the linkage method used was complete (farthest neighbour) because the individual characters are assumed to accumulate with age. Ontogenetic stages recognized by the cluster analysis could then be converted to percentage maturity values following the same procedure used for the parsimony-based stages.

It should be stressed that the percentage maturity values assigned to parsimony- and cluster-based ontogenetic stages are not meant to imply temporal equivalence in the length of stages. Designation of a bone as 50% mature, for example, does not necessarily equate to 'half grown' in a temporal sense, as different ontogenetic stages may have different durations with respect to the lifespan of the individual.

Date of death values

Known dates of death were converted from the recorded month–day format into single numerical values by the following procedure. Months were assigned consecutive whole number values (1 for January, 2 for February, etc.). Days were computed by dividing the actual day of death by the total number of days in the month. The resulting day value was added to the month value to produce the date of death value. A recorded date of death of 15 June, for example, would therefore be expressed as 6.5. One potential confusion results from these calculations. Because the day value for the last day of any month is always one, whole number date of death values actually represent death on the last day of the previous month, rather than the first day of the current month, as would be intuitively assumed. Thus, a date of death value of 2 represents death on 31 January not 1 February, and a death on 31 December receives a value of 13. Two ambiguous dates in the data set recoded as 'December' and 'late December' were estimated as follows: the former was assigned an arbitrary mid-month date of 15 December, the latter was assigned to 31 December.

Coding of surface textures

Bones were examined at the gross level and with a 10× hand lens under directed incandescent light. Textural features of all bones were documented qualitatively through a combination of detailed specimen notes, sketches, and photography. Observations were restricted to bone shafts; extreme proximal and distal ends were not considered due to the potential confounding effect of attachment areas for joint capsules and articular cartilage. Definitions of major textural types and textural coding of individual bones were based on recorded descriptions without any reference to skeletal maturity estimates. Femora, tibiotarsi, and humeri were analysed as separate subsamples. Bones within each subsample were grouped based on similar shaft textures, and textural features of these groupings defined textural types for that element. Textural types were placed in an ordered sequence based on decreasing shaft porosity; sequential types within the sequence were assigned sequential numerical values. Only after these values were established was the relationship between texture type and ontogeny examined.

Relationship between texture type and ontogeny

The relationship between bone surface texture and maturity was evaluated by visual inspection of texture type vs. size and percentage maturity plots. The significance of the relationship between texture type and size was determined by ANOVA. In addition, the relationship between texture and cluster-based ontogenetic stage was analysed using a two-way ranked-order contingency table. In addition to Pearson's chi-squared statistic, the values for Spearman's rho and Goodman–Kruskal's gamma statistics were also determined. Chi-squared tests whether the two categories are independent. Rho tests the same question using rank indices rather than actual data; it is thus independent of sample size influences. Gamma tests whether the prediction of the value of one category is

improved by knowledge of the other category. In cases where the number of ontogenetic stages was equal to the number of texture types, McNemar's test of symmetry was applied.

The auto-control study

In addition to the DMNH collection, a growth series of eight individuals was obtained from TSBR during May–November 2001. All birds were natural deaths, or were euthanized by TSBR due to their inability to further survive in the wild. At the time of death, both pelvic limbs were disarticulated at the hip joint and preserved intact. Right limbs were frozen and subsequently skeletonized in the DMNH dermestid beetle colony. Ontogenetic character states and detailed textural observations were recorded for femora and tibiotarsi following the procedures used for the DMNH skeletons. Left limbs were fixed in 10% buffered formalin and preserved in 70% ethanol until processing in February 2002. After the removal of most soft tissue, the femora and tibiotarsi were decalcified in 15% formic acid, rinsed and dehydrated in a graded series of ethanol, and embedded in paraffin wax. Thin sections, 5 μm thick, were cut and stained with Mayer's haematoxylin and eosin. The locations of the thin sections are shown in Figure 1. With reference to textural data collected from the contralateral elements, sections were examined by light microscopy to evaluate histological correlates of gross textural types, and to relate observed surface textures to the overall growth regime of *B. canadensis*. TSBR specimens used in the auto-control study were later accessioned into the DMNH collection.

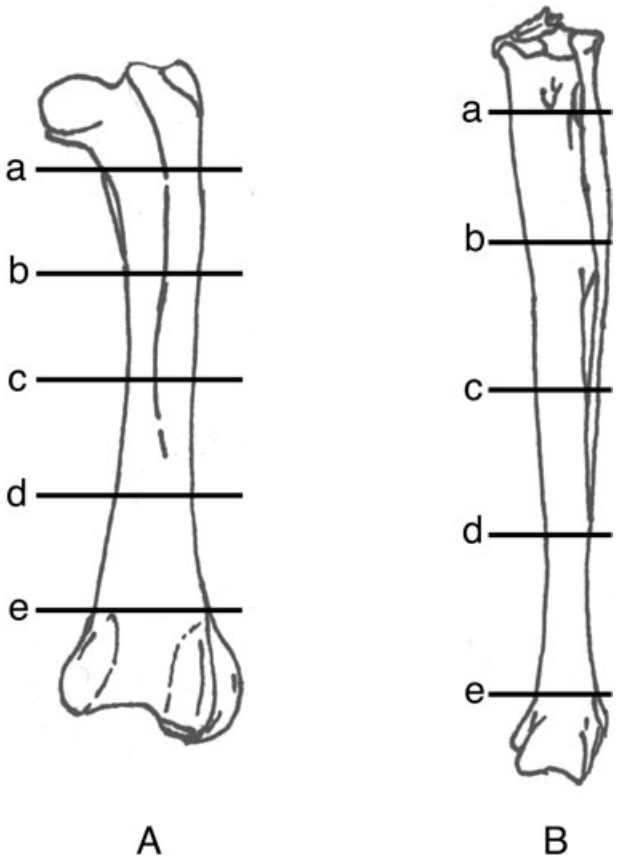

Figure 1. Locations of thin sections used in the auto-control study. A, femur; B, tibiotarsus. Labelled lines indicate the positions of transverse sections. Longitudinal sections are designated based on the transverse lines they intersect.

RESULTS

Size-independent maturity estimates

Strict consensus trees derived from parsimony analyses of femora, tibiotarsi, and humeri are shown in Figure 2. Not counting the outgroup stage lacking all characters (designated as stage 0 for all three elements), 12 ontogenetic stages were recognized for the femur, five for the tibiotarsus, and seven for the humerus. Parsimony-based ontogenetic stages are defined in Table 4. Character definitions for each stage are cumulative: stage 1 is defined by the presence of the characters listed, stage 2 by the presence of all the characters for stage 1 plus the defining characters of stage 2, and so on.

The results of the cluster analyses are shown in Figure 3; cluster-based ontogenetic stages are defined in Table 5. The ontogenetic stages shown in Figure 3 and defined in Table 5 represent stable portions of the clusters (a cluster level that does not change with different character additions). This is at distances > 0.10 in some cases. Individual DMNH 82688 was excluded from the cluster analyses due to anomalous combinations of character states not present in any other individuals. Excluding stage 0 lacking all characters, seven ontogenetic stages were recognized for the femur, six for the tibiotarsus, and seven for the humerus. As with the parsimony analysis, character acquisitions among stages are cumulative. Stages and defining characters are similar to those identified by the parsimony analysis (Table 4).

Femoral characters 5, 6, 10, and 12–16 appear to be part of a complex of muscle scars arising more or less simultaneously during cluster-based stages 4 and 5. The process generally seems to begin with the acquisition of character 5 (scar for M. tibialis cranialis) and ends with the acquisition of character 16 (scar for M. flexor perforans et perforatus II). The other characters in this complex appear at different times in different individuals, resulting in small differences in the clusters, especially within stage 4. This probably

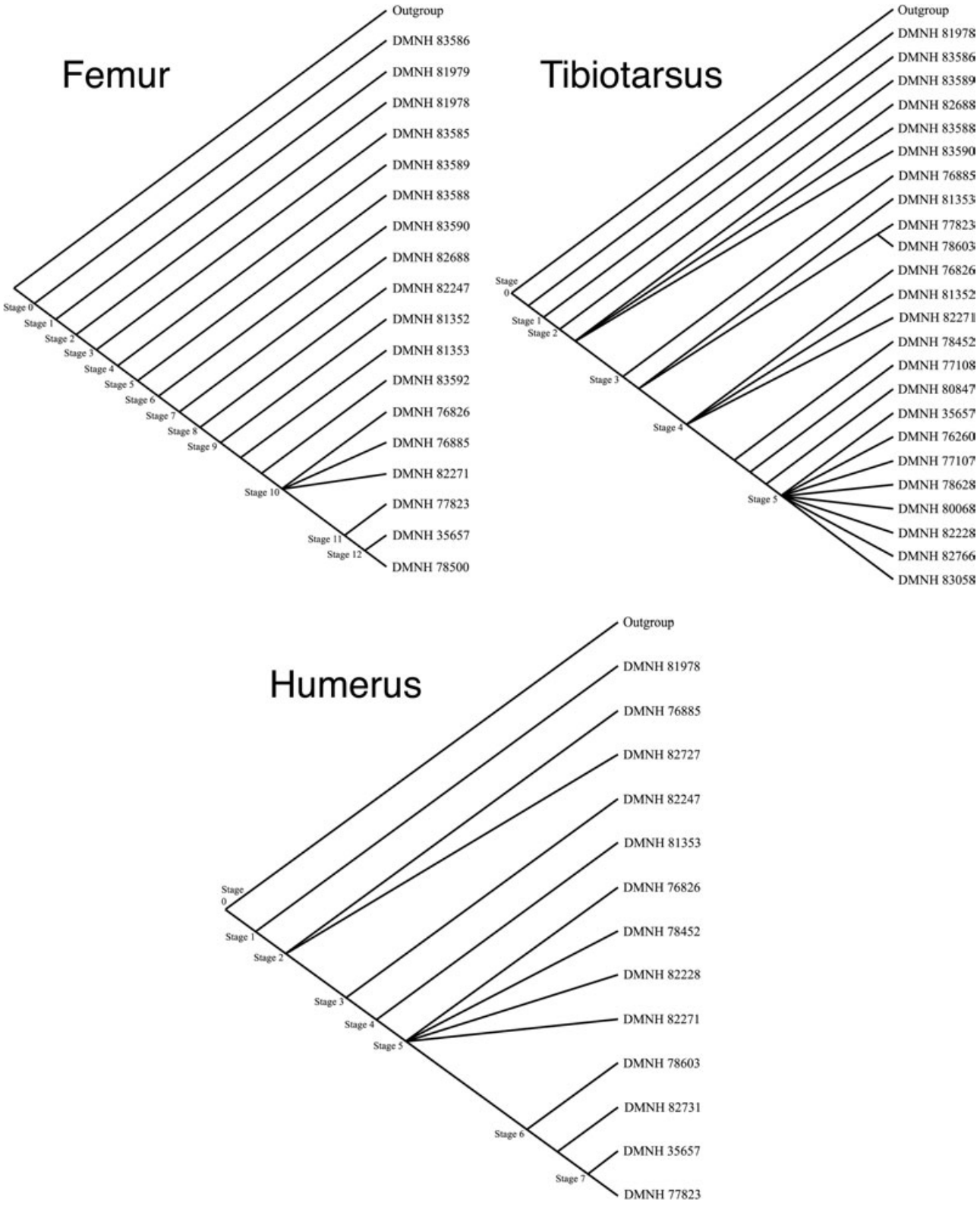

Figure 2. Strict consensus trees resulting from parsimony analyses. Numbered ontogenetic stages are defined in Table 4. Femur: strict consensus of four trees, tree length = 28, consistency index = 0.7500. Tibiotarsus: strict consensus of 40 trees, tree length = 31, consistency index = 0.6452. Humerus: strict consensus of six trees, tree length = 19, consistency index = 0.8333.

Table 4. Ontogenetic stages as determined by the parsimony analyses. The character acquisition is cumulative: stage 2 possesses the characters listed for stages 1 and 2, etc. The numbers in parentheses indicate the character numbers as listed in Appendix 1

Stage	Definition	Percentage maturity
Femur		
0	Absence of all coded characters	0
1	Appearance of:	
	Scar for M. puboischiofemoralis (8)	8
2	Appearance of:	
	Caudal intermuscular line (7)	17
3	Appearance of:	
	Bony distal condyles present (3, state 1)	25
4	Appearance of:	
	Bony femoral head present (1, state 1)	33
5	Appearance of:	
	Cranial intermuscular line (4)	42
6	Appearance of:	
	Crista tibiofibularis (11)	50
7	Appearance of:	
	Lateral collateral ligament impression (18)	58
8	Appearance of:	
	Bony greater trochanter present (2, state 1)	
	Scar for M. flexor perforans and perforatus III (17)	67
9	Appearance of:	
	Scar for M. tibialis cranialis (5)	75
10	Appearance of:	
	Scar for M. ischiofemoralis (14)	
	Lateral scar for M. iliotrochantericus cranialis and medius (15)	83
11	Appearance of:	
	Bony greater trochanter completely ossified (2, state 2)	
	Bony distal condyles completely ossified (3, state 2)	92
12	Appearance of:	
	Bony femoral head completely ossified (1, state 2)	100
Tibiotarsus		
0	Absence of all coded characters	0
1	Appearance of:	
	Crista fibularis (5)	20
2	Appearance of:	
	Tubercle for Mm. peroneus longus and brevis retinaculum (6)	40
3	Appearance of:	
	Bony proximal end present (1, state 1)	
	Cranial cnemial crest (7)	
	Lateral cnemial crest (8)	
	Proximal scars for M. extensor digitorum longus (9)	
	Scar for M. femorotibialis externus (12)	
	Scar for M. femorotibialis internus (14)	
	Complex of scars for M. gastrocnemius pars medialis, M. plantaris, and Mm. flexores cruri lateralis and medialis (15)	60
4	Appearance of:	
	Distinct scars for M. plantaris and Mm. flexores cruri lateralis and medialis (16)	80
5	Appearance of:	
	Bony proximal end completely ossified (1, state 2)	100

Table 4. *Continued*

Stage	Definition	Percentage maturity
Humerus		
0	Absence of all coded characters	0
1	Appearance of:	
	Bony deltopectoral crest (2)	14
2	Appearance of:	
	Fossa for M. brachialis (13)	29
3	Appearance of:	
	Bony humeral head present (1, state 1)	
	Bony distal condyles present (3, state 1)	
	Pneumatic foramen (6)	
	Dorsal tubercle (9)	
	Transverse ligamental groove (10)	43
4	Appearance of:	
	Scar for M. pectoralis (4)	
	Groove for M. humerotriceps tendon (8)	57
5	Appearance of:	
	Groove for M. scapulotriceps tendon (7)	71
6	Appearance of:	
	Bony humeral head fully ossified (1, state 2)	86
7	Appearance of:	
	Bony distal condyles fully ossified (3, state 2)	100

reflects natural individual variation, and such variability might also be discernible in the younger stages with a larger sample size. Stages 2–4 are defined by the acquisition of character suites; the order of acquisition of individual characters varies by individual within these stages. This has the result of collapsing several of the parsimony-based femoral stages (Table 4) into larger, more inclusive cluster-based stages (Table 5). Stage 1 is equivalent in both analyses. Cluster-based stage 2 encompasses parsimony-based stages 2, 3, and 4; cluster-based stage 3 encompasses parsimony-based stages 5 and 6; and cluster-based stage 4 encompasses parsimony-based stages 7, 8, and 9. Cluster-based stages 5, 6, and 7 are equivalent to parsimony-based stages 10, 11, and 12, respectively.

For the tibiotarsus, ontogenetic stages 2–6 recognized by the cluster analysis are identical to stages 1–5 based on the parsimony analysis (Tables 4, 5). The principal difference between the results of the two methods is the recognition by the cluster analysis of a stage 1 defined only by the presence of character 10 (extensor sulcus). This character is present in all individuals except DMNH 82688; the removal of that individual from the cluster analysis is responsible for the recognition of the additional stage. The end result of this is the separation of three individuals (DMNH 81978, DMNH 81979, DMNH 83585) from parsimony-based stage 1 (equivalent to cluster-based stage 2) into cluster-based stage 1.

The ontogenetic stages recognized by the cluster analysis of the humerus are identical to those based on the parsimony analysis (Tables 4, 5).

Figure 4 shows the relationships between the percentage adult size as calculated from element lengths and the percentage maturity as determined by the parsimony and cluster analyses. Overall, there is good correspondence between the size of the bones and ontogenetic status, although there appears to be somewhat more variability earlier in ontogeny. There is a weaker correspondence in bones less than 35% mature, probably a result of individual variation in growth rates during the rapid growth period of early ontogeny. For all three elements, individuals do not appear to reach 100% maturity below 89% adult size. [There is one exception on the tibiotarsus plots, where the bone exhibits full maturity at 69% adult size. On the basis of measurements of the other limb elements, this individual (DMNH 80059) appears to have had an unusually short tibiotarsus compared with the other birds examined. The bone has no other noticeable abnormalities.] Not all individuals at or above 89% adult size, however, exhibit full maturity. Figure 4 shows that the bones attain adult size before reaching full maturity, and therefore an adult-sized bone is not necessarily fully mature. Moreover, the degree of

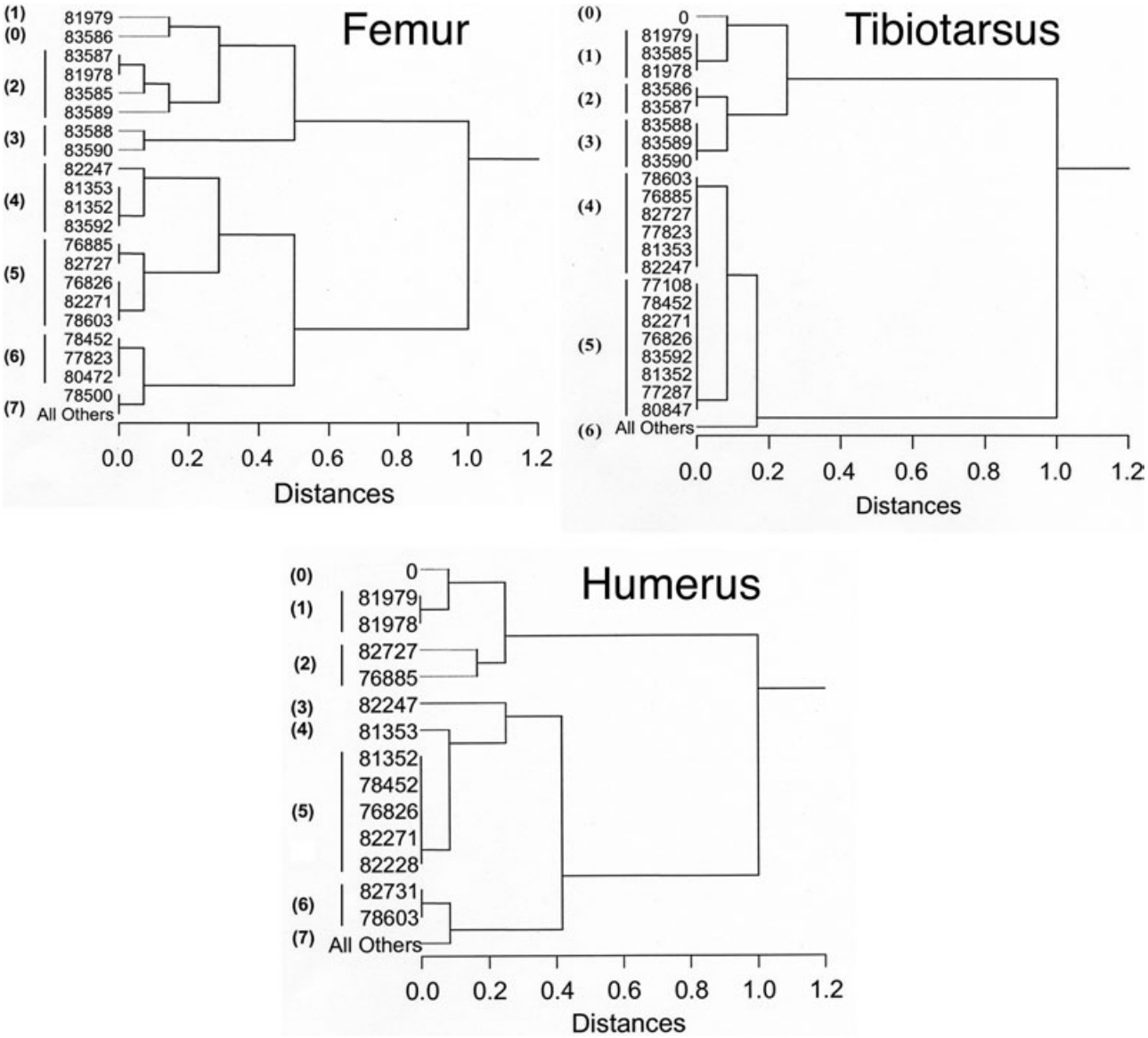

Figure 3. Results of the cluster analyses of bone landmark characters. The distance metric is normalized percent disagreement. Complete linkage method (farthest neighbour). All specimen designations are DMNH catalogue numbers. The numbers in parentheses represent ontogenetic stages. Femur: DMNH 78500 differs from 'All Others' only in the lack of character 10 (medial scar for M. flexor perforati II and IV). Tibiotarsus: DMNH 83058 differs from 'All Others' only in the lack of character 13 (peroneal sulcus). Humerus: DMNH 78603 differs from 'All Others' only in the lack of character 12 (bicipital crest).

maturity when adult size is reached varies by element, with femora and tibiotarsi generally maturing earlier than humeri.

TEXTURAL TYPES

Independent analyses of femoral, tibiotarsal, and humeral shafts revealed a suite of seven major textural classes common to all three elements. Each major type can be further divided into two subtypes, although not all subtypes are present in all elements. Texture types with their assigned numerical values are described below and summarized in Table 6. Unless expressly contrasted with a rugose pattern, the term 'grossly smooth' is here used to indicate a lack of visible surface porosity.

Type I

The entire shaft of type I bones is textured and rough to the touch. Proximal and/or distal shaft regions bear a conspicuous pattern of longitudinal striations,

Table 5. Ontogenetic stages as determined by the cluster analyses. The character acquisition is cumulative. The numbers in parentheses indicate character numbers as listed in Appendix 1

Stage	Definition	Percentage maturity
Femur		
0	Absence of all coded characters	0
1	Appearance of:	
	Scar for M. puboischiofemoralis (8)	14
2	Variable appearance of characters in suite:	
	Bony femoral head present (1, state 1)	
	Bony distal condyles present (3, state 1)	
	Caudal intermuscular line (7)	29
3	Variable appearance of characters in suite:	
	Cranial intermuscular line (4)	
	Crista tibiofibularis (11)	43
4	Variable appearance of characters in suite:	
	Bony greater trochanter present (2, state 1)	
	Scar for M. tibialis cranialis (5)	
	Scar for M. flexor perforans and perforatus III (17)	
	Lateral collateral ligament impression (18)	57
5	Appearance of:	
	Scar for M. ischiofemoralis (14)	
	Lateral scar for M. iliotrochantericus cranialis and medius (15)	71
6	Appearance of:	
	Bony greater trochanter completely ossified (2, state 2)	
	Bony distal condyles completely ossified (3, state 2)	86
7	Appearance of:	
	Bony femoral head completely ossified (1, state 2)	100
Tibiotarsus		
0	Absence of all coded characters	0
1	Appearance of:	
	Extensor sulcus (10)	17
2	Appearance of:	
	Crista fibularis (5)	33
3	Appearance of:	
	Tubercle for Mm. peroneus longus and brevis retinaculum (6)	50
4	Appearance of:	
	Bony proximal end present (1, state 1)	
	Cranial cnemial crest (7)	
	Lateral cnemial crest (8)	
	Proximal scars for M. extensor digitorum longus (9)	
	Scar for M. femorotibialis externus (12)	
	Scar for M. femorotibialis internus (14)	
	Complex of scars for M. gastrocnemius pars medialis, M. plantaris, and Mm.flexores cruri lateralis and medialis (15)	67
5	Appearance of:	
	Distinct scars for M. plantaris and Mm. flexores cruri lateralis and medialis (16)	83
6	Appearance of:	
	Bony proximal end completely ossified (1, state 2)	100
Humerus		
0	Absence of all coded characters	0
1	Appearance of:	
	Bony deltopectoral crest (2)	14
2	Appearance of:	
	Fossa for M. brachialis (13)	29

Table 5. *Continued*

Stage	Definition	Percentage maturity
3	Appearance of:	
	Bony humeral head present (1, state 1)	
	Bony distal condyles present (3, state 1)	
	Pneumatic foramen (6)	
	Dorsal tubercle (9)	
	Transverse ligamental groove (10)	43
4	Appearance of:	
	Scar for M. pectoralis (4)	
	Groove for M. humerotriceps tendon (8)	57
5	Appearance of:	
	Groove for M. scapulotriceps tendon (7)	71
6	Appearance of:	
	Bony humeral head fully ossified (1, state 2)	86
7	Appearance of:	
	Bony distal condyles fully ossified (3, state 2)	100

Table 6. Summary of texture types, subtypes, and assigned numerical values. Defining features of subtypes are indicated by italics

Texture type	Defining features	Numerical value
I	Longitudinal striations present	
	Lattice of transverse struts present	1.0
	Lattice of transverse struts absent	1.5
II	Longitudinal striations absent;	
	Entire shaft fibrous and/or porous	2.0
	Transverse wrinkling of surface present	2.5
III	Proximal and distal regions fibrous and/or porous;	
	Midshaft smoother with nonpenetrating dimples and/or longitudinal grooves	3.0
	Transverse wrinkling of surface present	3.5
IV	Nonpenetrating longitudinal surface grooves prevalent	
	Isolated patches of penetrating pores present	4.0
	Isolated patches of penetrating pores absent	4.5
V	Co-occurrence of nonpenetrating longitudinal surface grooves and smooth areas	
	Isolated patches of penetrating pores present	5.0
	Isolated patches of rough grainy surface without well-defined pores present	5.5
VI	Surface grossly smooth;	
	Isolated areas of faint longitudinal surface grooves	6.0
	Transverse wrinkling and/or rugose surfaces present	6.5
VII	Surface grossly smooth;	
	Longitudinally orientated textures absent	7.0
	Transverse wrinkling and/or rugose surfaces present	7.5

visible as a series of sharp parallel ridges and deep narrow furrows (Fig. 5A). Midshaft regions are grossly porous. Pores may penetrate the shaft obliquely with longitudinally orientated trailing surface grooves to create a fibrous appearance (Fig. 5B, C) or perpendicular to the bone surface to create a dotted pattern (Fig. 5D). Areas of rough grainy surface without clearly defined individual pores are occasionally encountered (Fig. 5E). Two subtypes may be defined: subtype 1.0 has transverse struts in portions of the striated regions, resulting in a lattice-like pattern; subtype 1.5 lacks these struts in all striated areas. (Subtype 1.5 is absent from the humerus sample.)

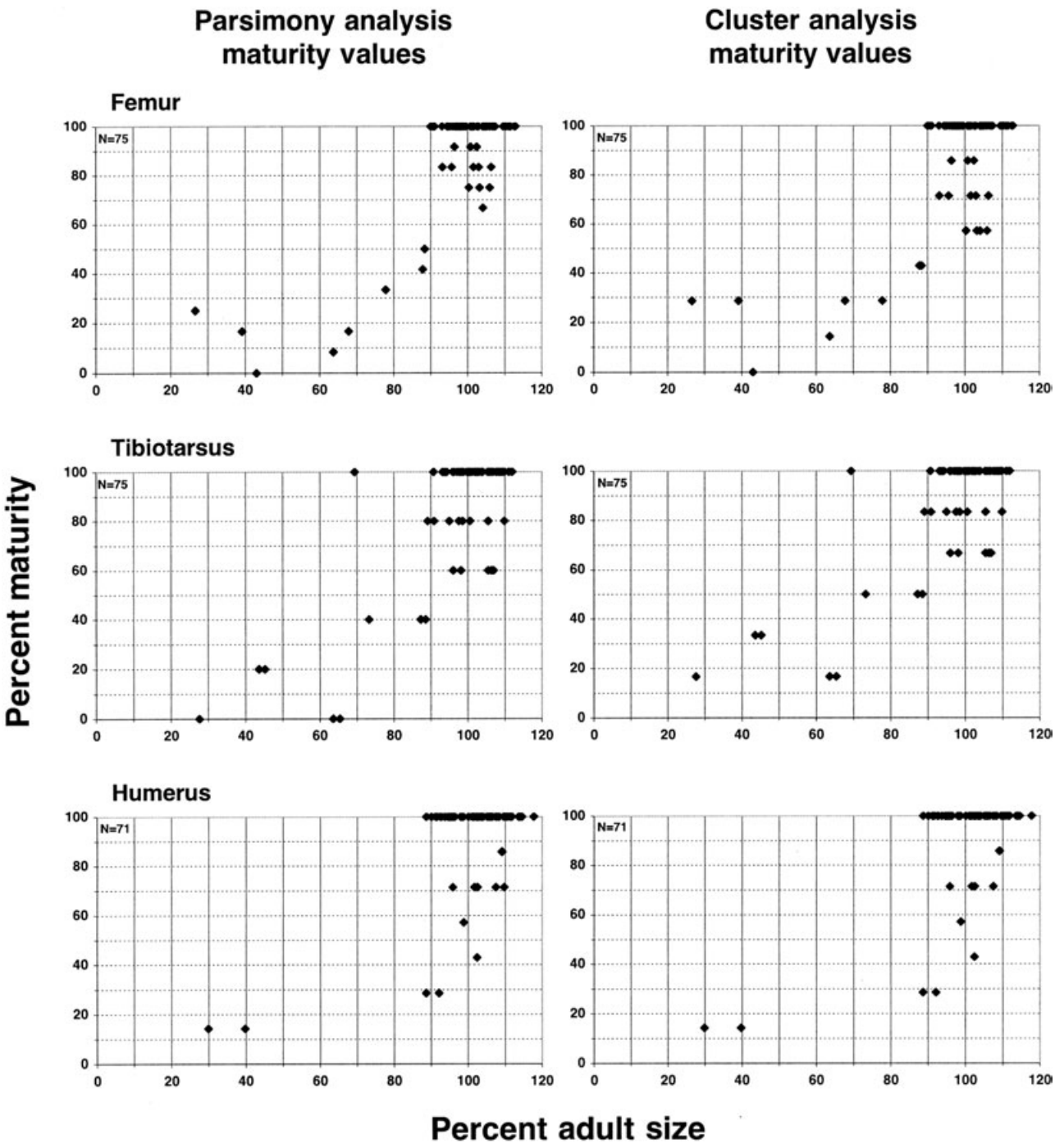

Figure 4. Relationships between the percentage adult size based on element length and the percentage maturity based on parsimony and cluster analyses.

Type II

Type II bones lack striated texture, but are otherwise similar to type I bones in that the entire shaft is textured and rough to the touch. Proximal, middle, and distal shaft regions exhibit the fibrous and/or porous patterns seen in the midshaft portions of type I bones. Two subtypes may be defined: subtype 2.0 has only the fibrous/porous longitudinal textures; subtype 2.5 has a faint pattern of transverse surface wrinkles (Fig. 6A, B) overprinting the longitudinal features. (Subtype 2.5 is present only in the femur sample.)

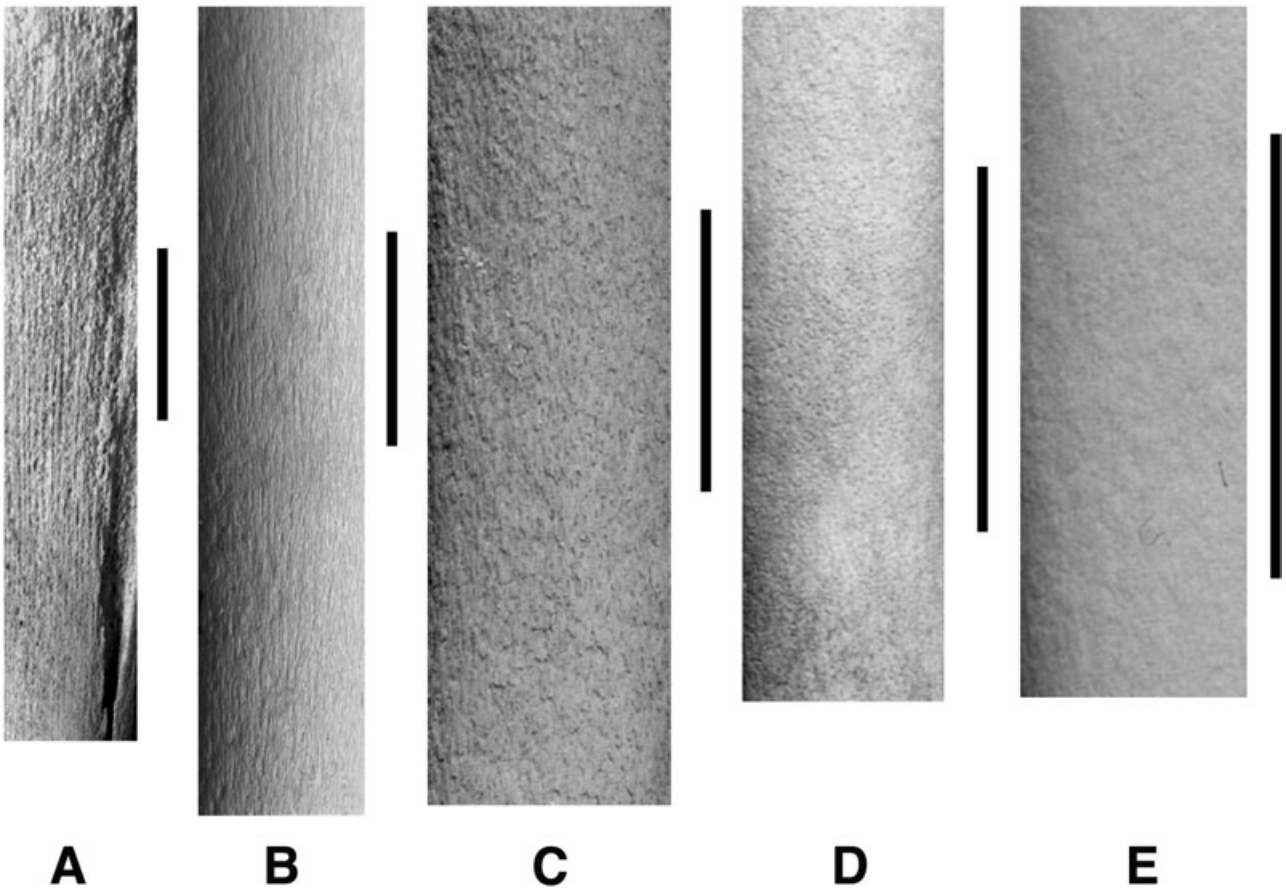

Figure 5. Examples of striated, fibrous, and porous texture patterns. A, longitudinal striations with (top) and without (bottom) transverse struts (DMNH 83589, tibiotarsus). B, fibrous texture (DMNH 78603, humerus). C, shorter-grained fibrous texture, intermediate between (B) and (D) (DMNH 82727, humerus). D, dotted pattern of porous texture (DMNH 82727, femur). E, rough grainy texture lacking distinct individual pores (DMNH 82247, femur). Scale bars = 1 cm.

Type III

Type III bones retain the rough textures of type II bones in the proximal and distal regions, but are smoother midshaft. Close examination of the midshaft region reveals a surface marked by shallow dimples and longitudinally directed grooves. However, these features differ from the striated and fibrous patterns by a lack of association with pores that penetrate the bone wall (Fig. 7A, B). Two subtypes may be defined: subtype 3.0 has only longitudinal textures; subtype 3.5 has occasional transverse wrinkles overprinting the longitudinal textures. (Subtype 3.5 is present only in the tibiotarsus sample.)

Type IV

The entire shaft of type IV bones is relatively smooth grossly, but close examination with a 10× hand lens reveals that most of the shaft is covered with nonpenetrating longitudinal textures, as in the midshaft regions of type III. Two subtypes may be defined: subtype 4.0 has isolated areas of scattered pores on the shaft (Fig. 6C); subtype 4.5 lacks this porosity. (Subtype 4.5 is present only in the humerus sample.)

Type V

Type V bones are for the most part grossly smooth. Examination with a 10× hand lens reveals a combination of completely smooth areas (Fig. 7C, D) and areas of nonpenetrating longitudinal textures, as in type IV. Some transverse wrinkling (Fig. 6A, B) may occasionally be present. Two subtypes may be defined: subtype 5.0 has occasional isolated patches of scattered porosity (Fig. 6C) on the shaft; subtype 5.5 has occasional patches of rough grainy surface without clearly defined pores. (Type V is completely absent from the humerus sample. Subtype 5.0 occurs

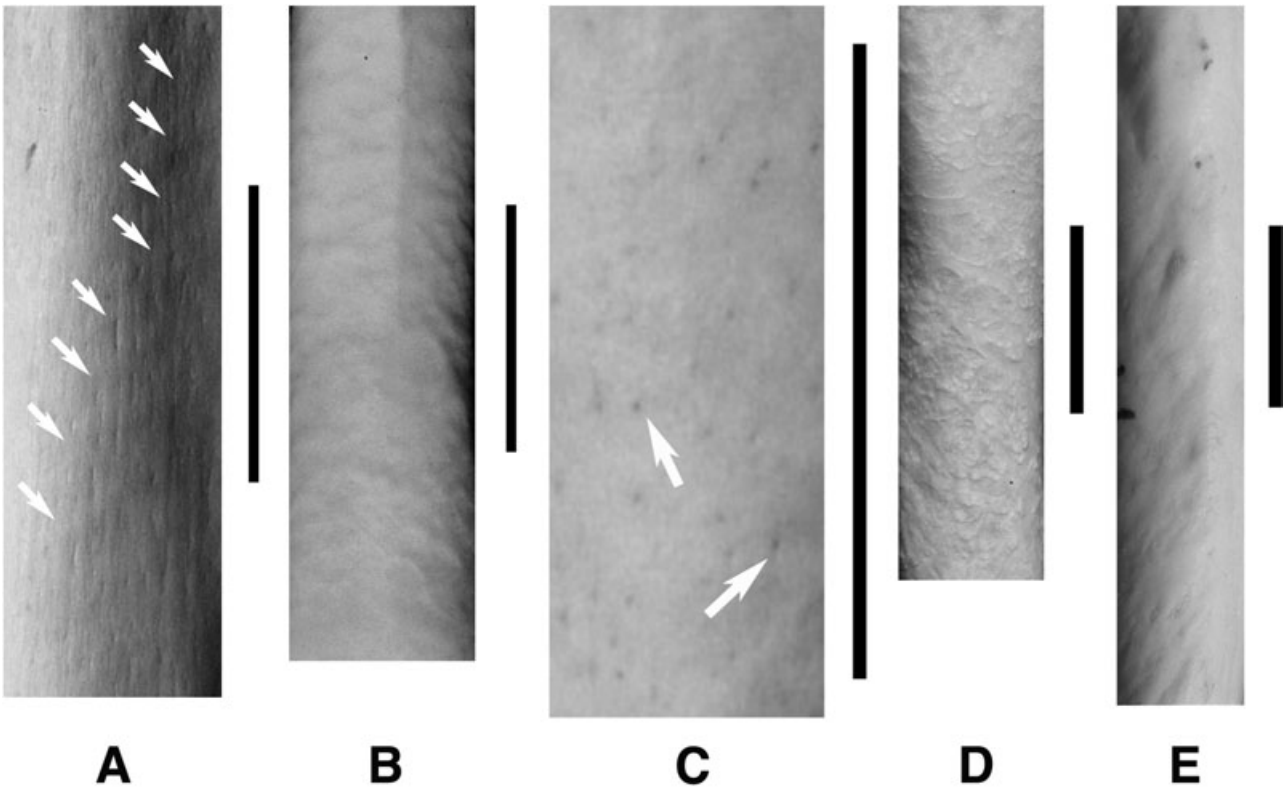

Figure 6. A, very faint transverse wrinkles, indicated by arrows (DMNH 82228, tibiotarsus). B, a more prominent transverse wrinkled texture pattern (DMNH 82910, femur). C, scattered pores, examples indicated by arrows, on an otherwise nonporous surface (DMNH 82729, femur). D, rugose texture (DMNH 82944, femur). E, areas of rugose texture on an otherwise smooth surface (DMNH 80847, humerus). Scale bars = 1 cm.

only in the tibiotarsus sample; subtype 5.5 only in the femur sample.)

Type VI

Type VI bones are grossly smooth. Examination with a 10× hand lens reveals a generally smooth shaft with sporadic faint occurrences of nonpenetrating longitudinal textures (Fig. 7C). Penetrating porosity is absent from the shaft. Two subtypes may be defined: subtype 6.0 has only smooth areas and longitudinal textures; subtype 6.5 has occasional surface rugosity and/or transverse wrinkling overprinting grossly smooth areas (Fig. 6A, B, D, E).

Type VII

Type VII bones are grossly smooth. All longitudinally directed textures are absent. Two subtypes may be defined: subtype 7.0 is completely smooth, even when examined under a 10× hand lens; subtype 7.5 has rugose areas and/or transverse wrinkling (Fig. 6A, B, D, E) in addition to smooth areas. (Subtype 7.0 is absent from the tibiotarsus sample.)

Relationship of surface textures to skeletal maturity

DMNH 82688 was excluded from the textural analyses because it lacked date of death data and thus could not always be compared with the rest of the sample. Figure 8 shows plots of texture type vs. element length and percentage adult size for all other individuals. Type I texture occurred throughout most of the size range examined, up to a maximum size of 88% (72 mm length) in the femur, 105% (159 mm length) in the tibiotarsus, and 102% (177 mm length) in the humerus. Types II–VII occurred only within the probable adult size range, confined to bones above 90% adult size (73 mm length) for the femur, 89% (153 mm length) for the humerus, and 89% (134 mm length) for the tibiotarsus. (The short tibiotarsus of DMNH 80059 was the only exception, on which type VI texture occurred at 69% adult size.) For all elements, within each of the seven major textural types, subtypes overlapped considerably in their size ranges, and did not provide any significant insights. The presence or absence of the transversely wrinkled pattern, in particular, had little diagnostic value, as it occurred

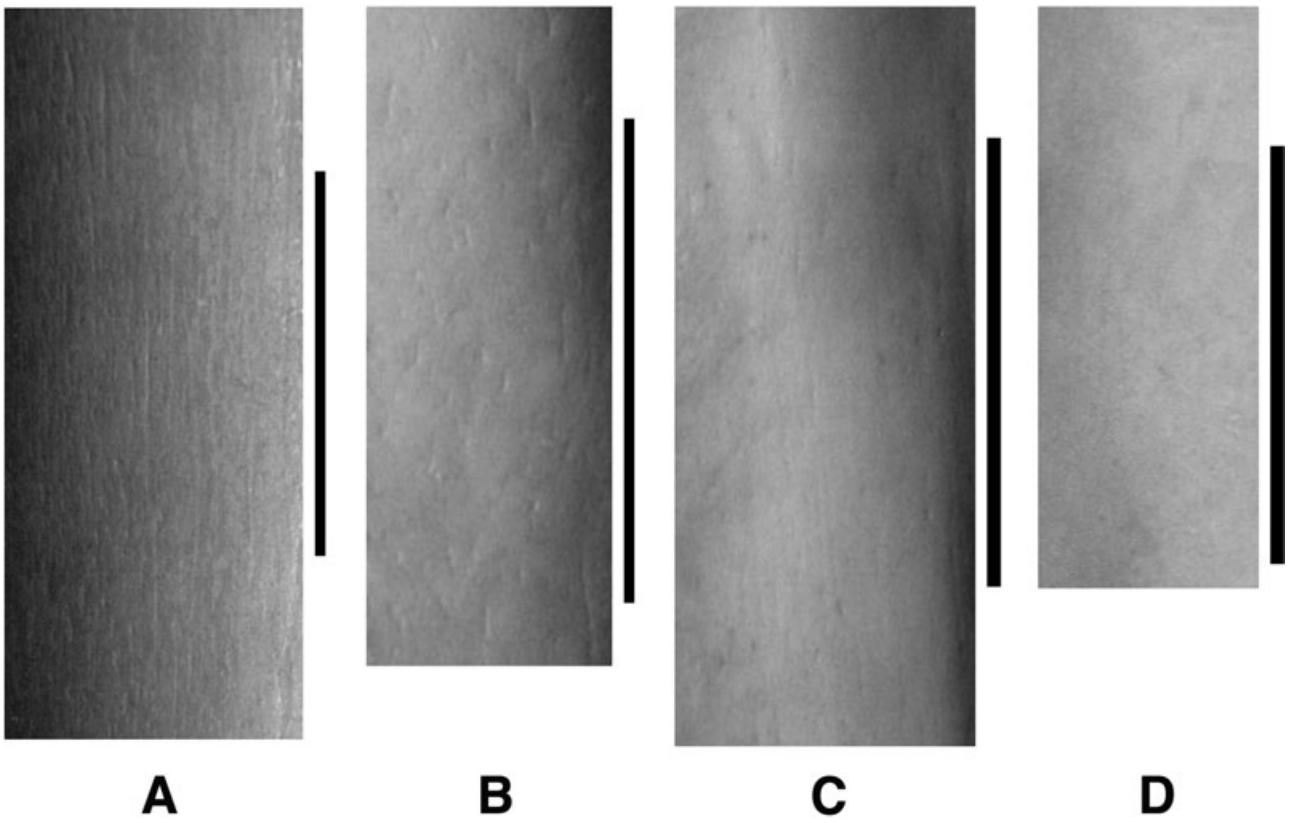

Figure 7. Examples of nonpenetrating longitudinal and smooth texture patterns. A, shallow longitudinal grooves (DMNH 82732, humerus). B, shallow surface dimples (DMNH 82730, femur). C, generally smooth texture with extremely faint longitudinal grooves (DMNH 82730, tibiotarsus). D, completely smooth surface (DMNH 82730, humerus). Scale bars = 1 cm.

sporadically in representatives of five texture types (types II, III, V, VI, and VII).

Figure 8 suggests that bones reach adult size ranges while still exhibiting type I texture, after which they progress through the other textural types on their way to full maturity. As determined by ANOVA, this pattern was statistically significant at $P < 0.05$ for all three subsamples. The mean length of bones with texture type I was significantly different from that of bones with texture types III–VII in all three elements; in the tibiotarsus and humerus it was also significantly different from that of bones with texture type II.

Size-independent plots of texture type vs. parsimony and cluster-based percentage maturity values (Fig. 9) provided better resolution and illustrated the disconnection between size and maturity. The overall pattern of texture distributions was similar for both the parsimony and cluster-based maturity indices, although actual percentage maturity values differed in the femur and tibiotarsus subsamples due to the differing number of ontogenetic stages recognized by the two size-independent methods. In the femur subsample, type I texture occurred only on bones less than 50% mature, although these same elements may be up to 90% adult size (Fig. 8). Texture types II and III formed distinct groupings between 67 and 92% mature (parsimony-based index) and 57 and 86% mature (cluster-based index). Type VII was confined to completely mature bones, as were all but two occurrences of type VI. Types IV and V only occurred in fully mature bones as well, but this may very well reflect the limited number of elements (one for type IV, two for type V). The relationship between texture type and percentage maturity was somewhat less clear for the tibiotarsus and humerus than for the femur; however, certain points were of interest. In the tibiotarsus subsample, texture type I was restricted to 60% (parsimony index) or 67% (cluster index) maturity and below, and was the only type to occur on bones less than 60% mature. Type VII and all but two occurrences of type VI occurred in fully mature bones. The single type V bone was also fully mature. The intermediate range from 60 (parsimony index) or 67 (cluster index) to 100% mature was occupied largely by texture types II–IV. In the humerus subsample, as for

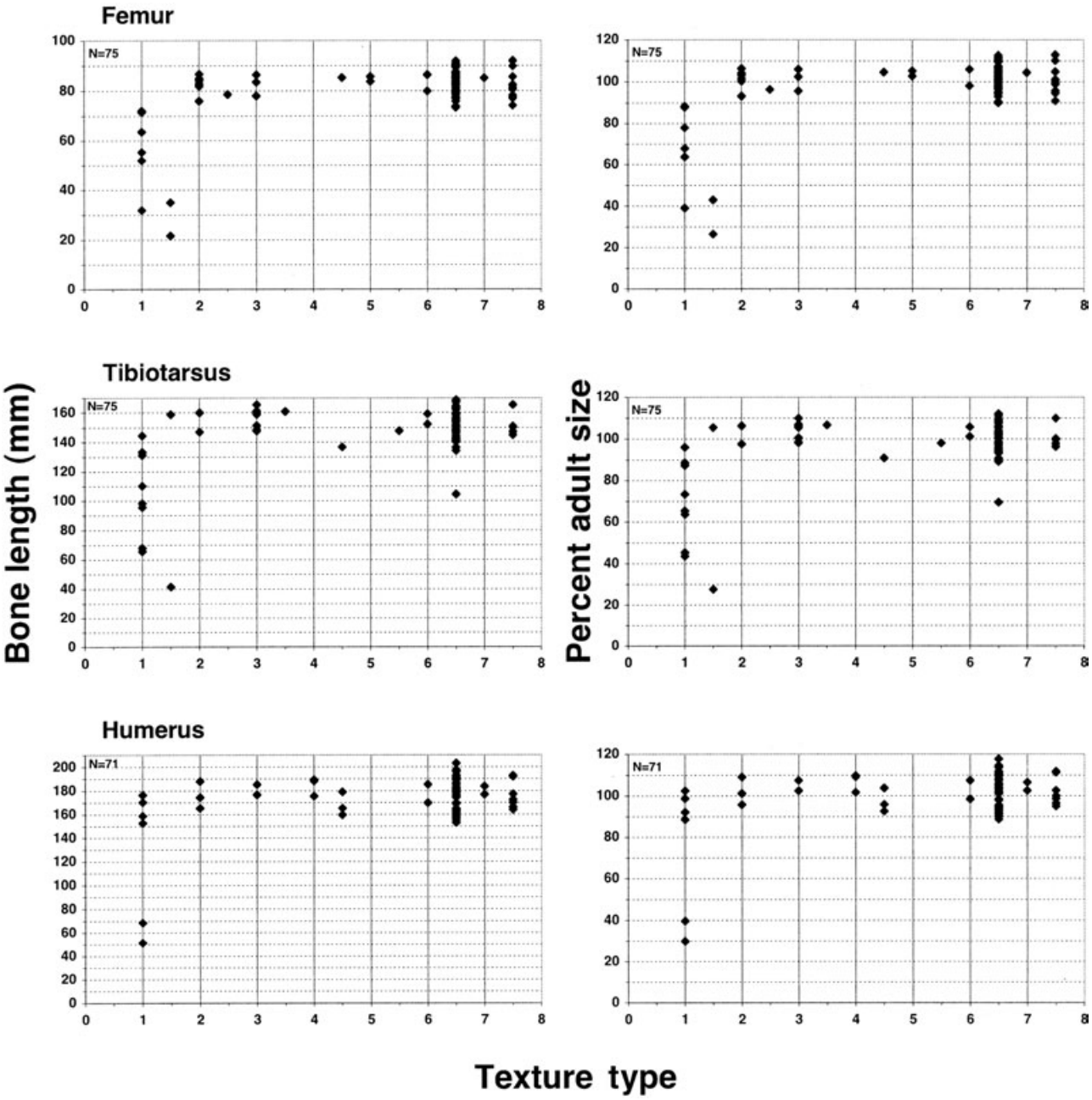

Figure 8. Relationships between texture type and bone length and percentage adult size.

the tibiotarsus, type I was the only texture type occurring in bones below 60% mature, and it was absent on more mature bones. Types II–IV occupied the intermediate 71–100% maturity range. Types VI and VII were restricted to fully mature bones.

Examination of the relationship between texture type and date of death (Fig. 10) further revealed that types I–V were temporally constrained. Occurrences of type I were confined to the period from May to July (femur) or August (tibiotarsus and humerus). Types II–V occurred only from late June (femur) or July (tibiotarsus and humerus) to November and were completely absent from all elements from December to May. There was much temporal overlap between occurrences of types II–V, and the pattern varied among elements such that it was difficult to identify a clear progression among these types. In general, though, types II and III were present from July (late June in the femur) to August (early September in the tibiotarsus) and types IV and V were present from

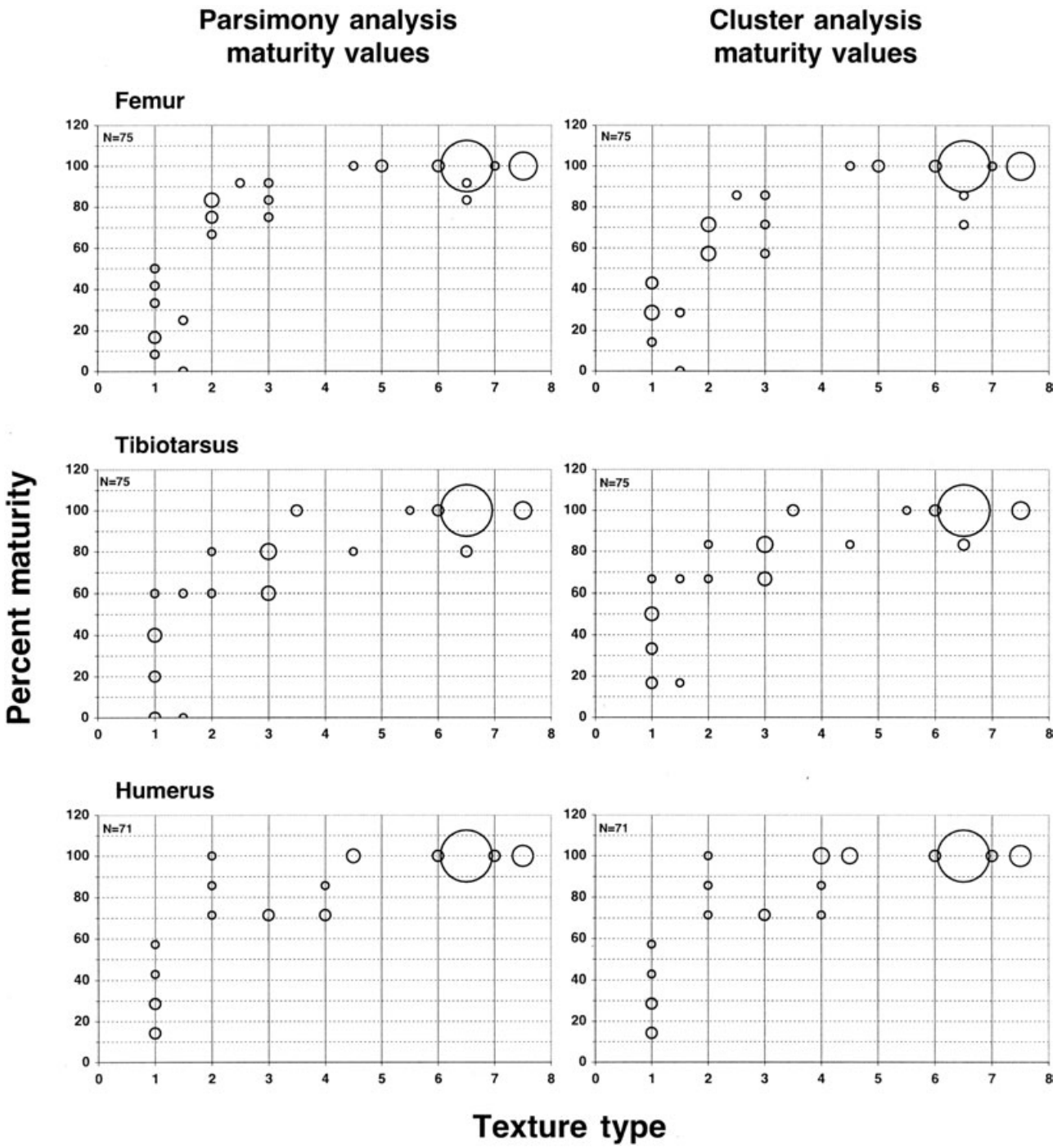

Figure 9. Relationships between texture type and parsimony-based and cluster-based percentage maturity indices. The circle diameter is proportional to the number of specimens.

August to November. In all elements, types II and III had their first appearances earlier in the year than types IV and V, and the latter persisted later. Unlike types I–V, texture types VI and VII occurred throughout the year. Given the correspondence of more porous texture types with less mature individuals (Fig. 9), the general configuration of the Figure 10 plots suggests an association of texture type I with newly hatched goslings in May, which then mature through texture types II–V before reaching skeletal maturity with texture type VI and/or VII by late November.

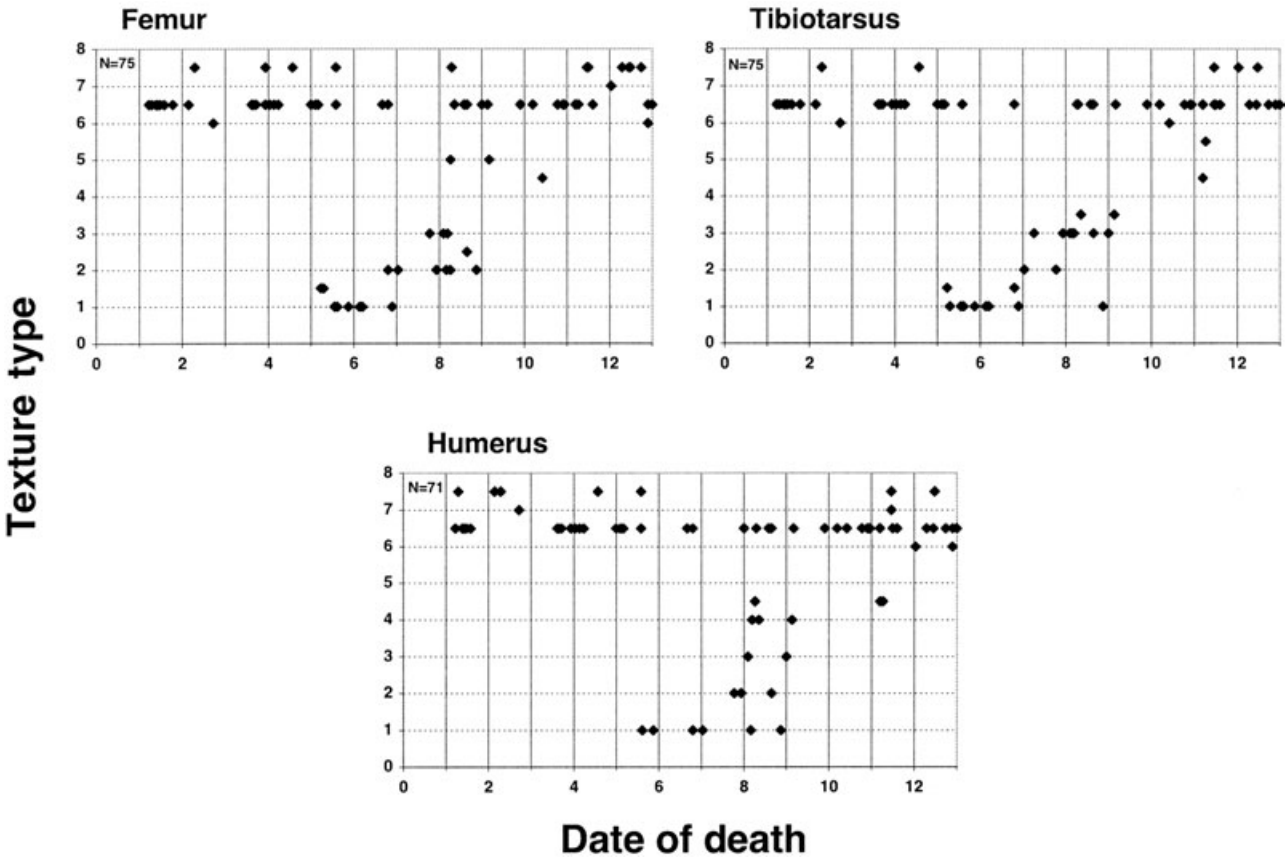

Figure 10. The relationship between texture type and date of death.

Table 7. Results of the statistical analyses of the relationship between texture type and cluster-based ontogenetic stage

Element	Statistic	Coefficient	Asymptotic error	Degrees of freedom	*P*-value
Femur	X^2	139.90		36	< 0.005
	McNemar's X^2	60.0		20	< 0.005
	ρ	0.80	±0.04		
	γ	0.98	±0.01		
Tibiotarsus	X^2	139.90		36	< 0.005
	ρ	0.87	±0.04		
	γ	0.99	±0.01		
Humerus	X^2	128.70		25	< 0.005
	McNemar's X^2	58		15	< 0.005
	ρ	0.76	±0.06		
	γ	0.98	±0.02		

The results of the statistical analyses of the two-way ranked-order contingency table to evaluate the relationship between texture and cluster-based ontogenetic stage are shown in Table 7. The chi-squared values confirmed that the two variables were not independent. In cases where the number of texture types and ontogenetic stages was the same (femur and humerus), McNemar's chi-square tested the symmetry of the data matrix by ignoring the diagonal and testing the upper and lower triangles of the matrix against each other. The result indicated that the two halves of the matrix were dissimilar, as would be expected if the earlier ontogenetic stages had no association with later (less porous) texture types. The values for rho and gamma were both very close to 1.0 with small standard errors. Rho further confirmed

that there was a strong association between ontogenetic stage and texture type, based on rank and independent of sample size influences. The gamma value indicated that knowledge of the ontogenetic stage may be reasonably used to predict texture type, and vice versa.

There was some suggestion that, within individuals, the more porous texture types may persist longer on the humerus than on the femur and tibiotarsus. This was seen in the persistence of, for example, type I textures at larger body sizes and later dates in the humerus (Figs 8, 10). Moreover, of 20 individuals for which all three elements were present and at least one element exhibited a texture type lower than type VI, 13 had humeri with a texture type lower than that of one or both hindlimb elements (Table 8). A similar observation was reported by Serjeantson (2002), who, based on the examination of four skeletons of *Anser*, noted more rapid maturation of the legs relative to the wings and body.

Histological correlates of surface features

The cortex of immature (juvenile and subadult) femora and tibiotarsi is composed of fibrolamellar bone (*sensu* de Ricqlès, 1974, 1976) containing numerous channels (Fig. 11). Channels contain blood vessels, identified by the presence of erythrocytes and/or endothelial vessel walls, as well as connective tissue and occasional lymphatic vessels (Fig. 11B). Rough surface patterns with penetrating porosity (striated, fibrous, porous) are gross expressions of intersections between channels and the periosteal bone surface. As the bone grows in width, channels are gradually roofed over by osteoid matrix and incorporated into the cortex (Fig. 11B, C). Once a channel is closed over, successive bony laminae are deposited within it, eventually restricting the channel lumen and forming a primary osteon with a central canal in which run the blood and lymphatic vessels. This results in a stratification of the bony cortex when viewed under low magnification, with stacks of channels that become progressively smaller in diameter and more recognizable as primary osteons as one moves away from the periosteal surface towards the medullary cavity (Fig. 11C). [Similar stratification has been recognized in the ostrich *Struthio camelus* and emu *Dromaius novaehollandiae* (Castanet *et al*., 2000), the Japanese quail *Coturnix japonica* (Starck & Chinsamy, 2002), and the mallard *Anas platyrhynchos* (de Margerie, Cubo & Castanet, 2002).]

The presence of a given surface pattern is largely controlled by channel orientation. Where channels are primarily longitudinal, striated texture results. Where channels are more oblique, and intersect the bone surface at an angle, the surface expression is more fibrous or porous. Oblique channels may be angled in a primarily longitudinal direction, or may have a circular (circumferential) orientation (Fig. 11D). In transverse section, longitudinally oblique channels may appear more elliptical than the more strictly longitudinal channels (Fig. 11C). This distinction is often quite subtle, however, and may not always be reliable if the plane of section deviates from a perfect transverse orientation. Longitudinal and oblique channels are more readily differentiated in longitudinal section (Fig. 12). In keeping with the grossly observed distributions of striated vs. fibrous texture, strongly oblique channels were more common in the middle third of the shafts of the youngest and smallest bones, and in the proximal and distal regions of older and larger bones. In midshaft sections of the youngest bones with a percentage maturity of zero, the cortex consisted of more spongy bone with a disorganized structure in longitudinal section (Fig. 12C). Channels were large and had little preferred orientation. Moving proximally and distally, channels became more regular and graded from oblique to longitudinal as extremities were approached (Fig. 12A, B). This corresponded to a grossly observed striated to fibrous to porous gradient from the ends to the midshaft.

Table 8. Texture types by element for individuals for which all elements are known and at least one element has a texture type below type VI. Asterisks indicate those individuals in which the texture of the humerus lags behind one or both hindlimb bones

Individual	Femur	Tibiotarsus	Humerus
DMNH 81978	I	I	I
DMNH 81979	I	I	I
DMNH 82688	I	I	I
DMNH 76885	II	I	I*
DMNH 82727	II	I	I*
DMNH 82247	II	II	I*
DMNH 81353	II	III	I*
DMNH 77823	II	III	II*
DMNH 78603	II	III	II*
DMNH 76826	III	II	II*
DMNH 81352	III	III	III
DMNH 78452	III	III	IV
DMNH 79340	IV	VI	VI
DMNH 82732	V	VI	IV*
DMNH 82729	V	VI	VI
DMNH 82271	VI	III	III*
DMNH 82228	VI	III	IV*
DMNH 82731	VI	III	IV*
DMNH 77108	VI	IV	IV*
DMNH 78500	VI	V	IV*

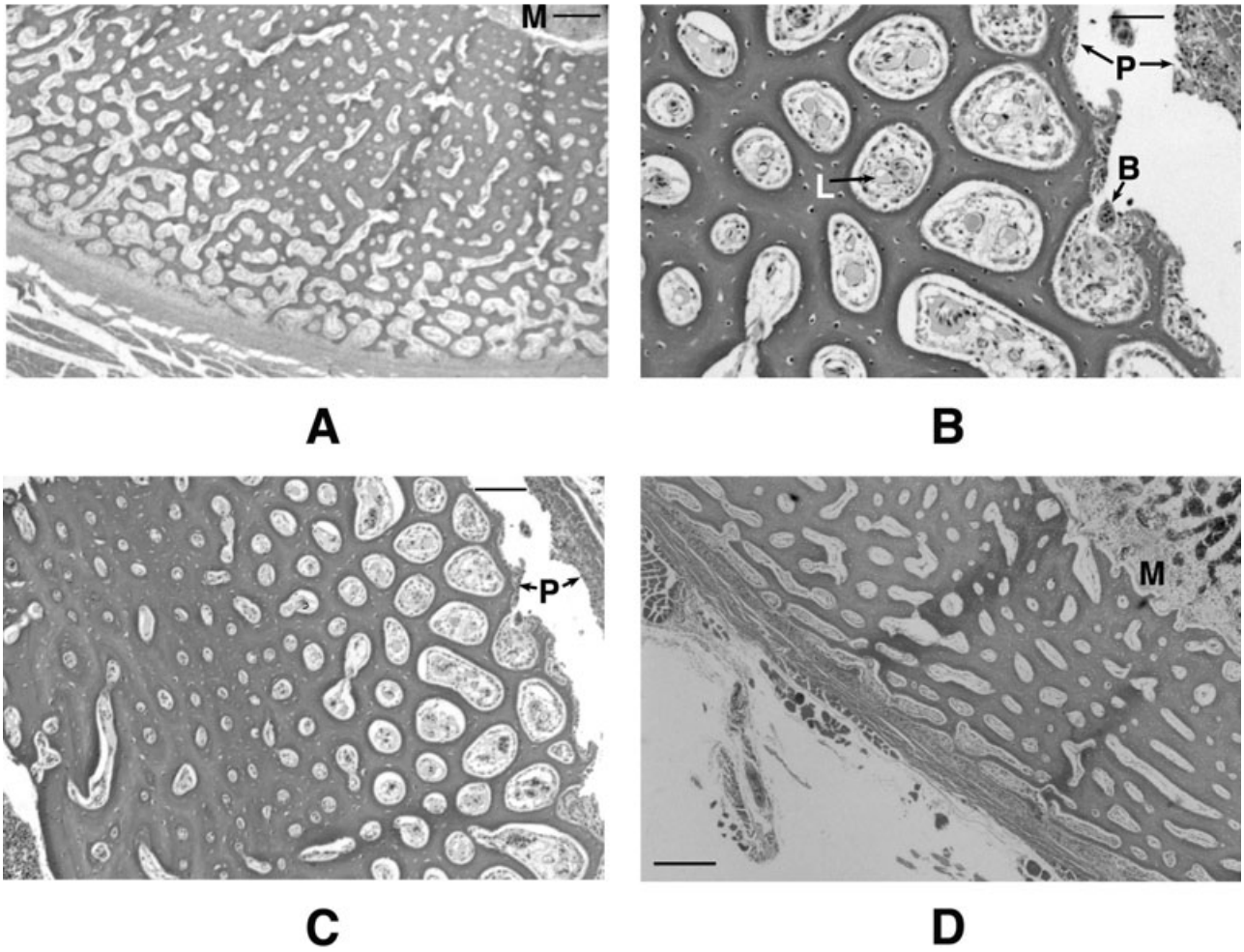

Figure 11. Transverse sections of immature long bones. A, single-layered fibrolamellar cortex (DMNH 83586, femur section c). B, active incorporation of channels at the surface of the fibrolamellar cortex (DMNH 83586, tibiotarsus section c). C, stratified fibrolamellar cortex (DMNH 83586, tibiotarsus section c). D, circularly orientated oblique channels in outer regions of fibrolamellar cortex (DMNH 83589, femur section d). B, blood vessel with erythrocytes; L, lymphatic vessel; M, medullary cavity; P, osteogenic layer of periosteum. The space within P is a preparation artefact. Scale bars: A, D = 230 μm; B = 50 μm; C = 92 μm.

Nonporous surface textures corresponded to a great reduction or absence of channels intersecting the bone surface. There was no histological distinction between completely smooth surfaces and those with nonpenetrating longitudinal grooves and/or dimples. In both these cases, surface expression of channels was extremely rare, if present at all. Nonporous textures were associated with two histological patterns in the elements examined (Fig. 13). In the midshaft regions of the tibiotarsus of DMNH 83592 (texture type III), grossly smooth surfaces were underlain directly by fibrolamellar bone; however, only an occasional channel penetrated the bone surface (Fig. 13A). In contrast, the femoral cortex of DMNH 83591 (texture type VI) exhibited a three-layered structure in which a central fibrolamellar region was enclosed by layers of low-vascularity lamellar bone periosteally and endosteally. In this case, the periosteal region of lamellar bone underlay the grossly smooth surface (Fig. 13B). In both cases, smooth surface textures were associated with a reduction in active bone deposition shown by the reduction of the inner osteogenic layer of the periosteum to a single layer of osteoblasts (Fig. 13A), as compared with its thicker condition in sections with active bone deposition and channel incorporation (Fig. 11C).

All textural features with clear histological correlates were associated with growth-related bone deposition, or lack thereof in the case of the smoother textures. Resorption at the periosteal surface associated with growth-related remodelling was also evident in some sections of immature bone. Resorptive

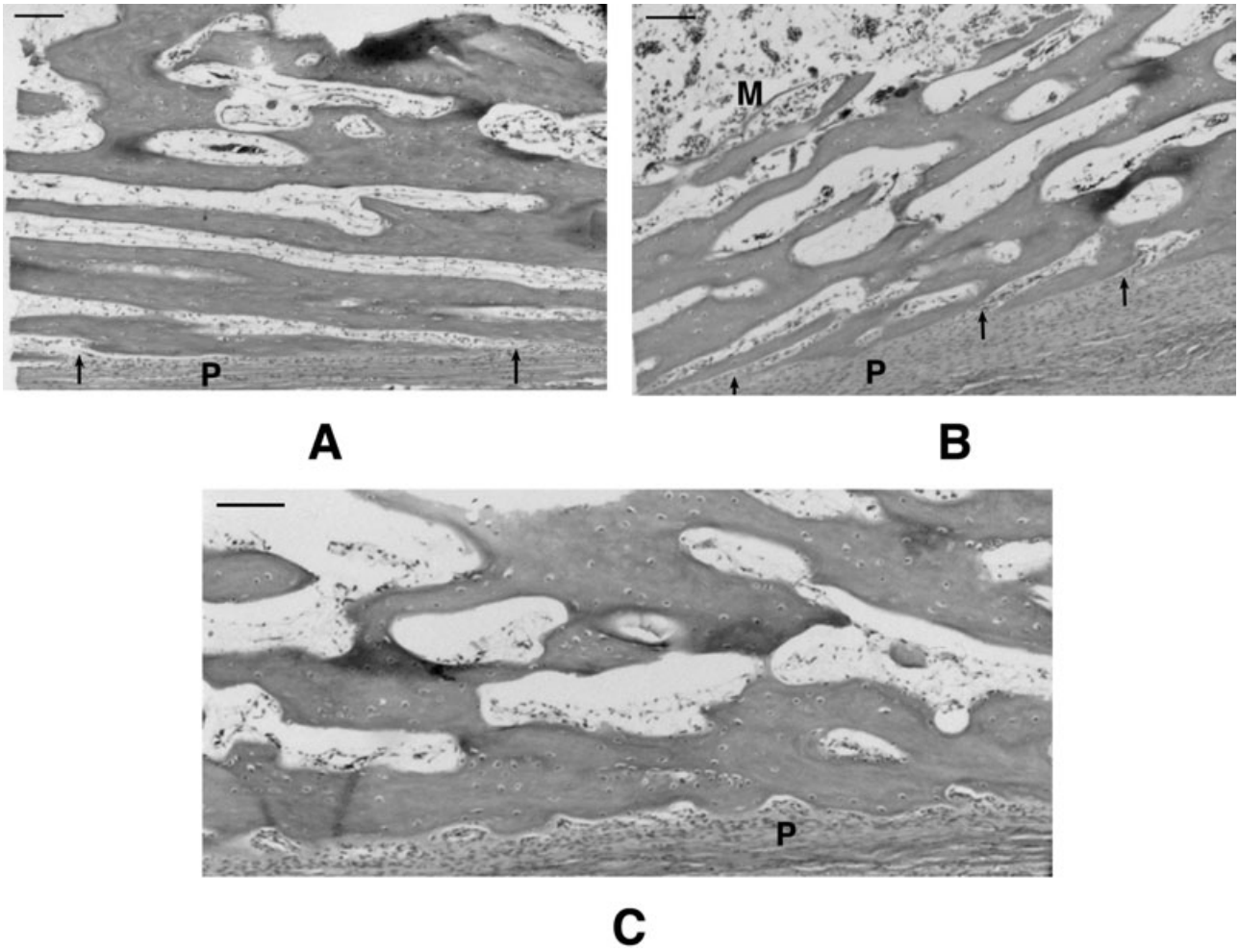

Figure 12. Juvenile bone DMNH 83585 in longitudinal section. A, longitudinal to slightly oblique channels intersecting the bone surface (arrows) in the distal region of the shaft (tibiotarsus region d). B, oblique channels intersecting the bone surface (arrows) just proximal to the midshaft region (tibiotarsus region b). C, irregular channels in the midshaft region (tibiotarsus region c). M, medullary cavity; P, periosteum. Scale bars = 92 μm.

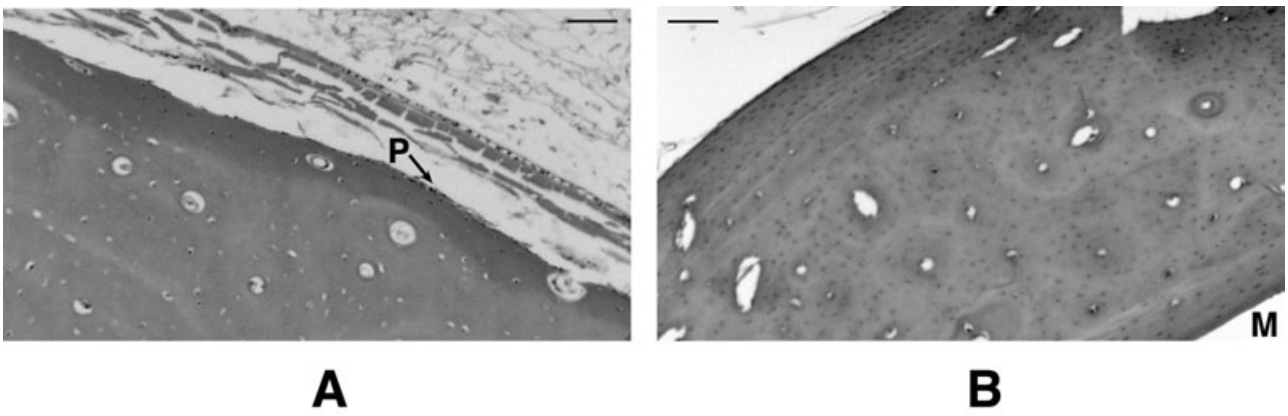

Figure 13. Histology underlying grossly smooth surface textures in transverse section. A, single-layered fibrolamellar cortex (DMNH 83592, tibiotarsus section c). B, three-layered cortex with a central fibrolamellar core and endosteal and periosteal lamellar bone (DMNH 83591, femur section e). M, medullary cavity; P, osteogenic layer of periosteum. Scale bars: A = 50 μm; B = 92 μm.

surfaces were characterized by highly irregular margins with large erosion bays, and the presence of numerous osteoclasts (Fig. 14). These features did not appear to be associated with any distinct gross textural pattern.

DISCUSSION

Hanson (1965, 1967) separated giant Canada geese (*B. c. maxima*) into age classes based on characters of the plumage, cloaca, and reproductive organs (oviduct and penis). During the autumn and winter period, he distinguished three age classes: immature (5–8 months), yearling (17–20 months), and adult (older than 29 months). In the spring and summer, he recognized four classes: gosling, yearling, 2-year-old adult, and old adult (the last not always distinguishable from 2 year olds). The osteological characters and textural types used in the present study distinguished three relative age classes, none of which directly corresponded to Hanson's divisions. These are here designated as juvenile, subadult, and adult. All juveniles and early subadults fell within Hanson's spring and summer gosling class; later subadults and the youngest adults fell within the autumn and winter immature class. All birds in the present study were skeletally mature by their first winter. Therefore, Hanson's (1965, 1967) older age classes could not be distinguished by the criteria employed here.

Juveniles are hatching-year birds that have not yet reached the adult size range. Juvenile bone invariably exhibits type I texture, identified by coarse, longitudinally directed striations. This texture seems to be equivalent to the lineations and spongy bone described by Callison & Quimby (1984) in immature *Struthio*, *Pterocnemia*, *Rhea*, *Casuarius*, *Meleagris*, and *Gallus* up to 75% adult size. Striated texture is usually concentrated on the proximal and distal thirds of the bone shaft.

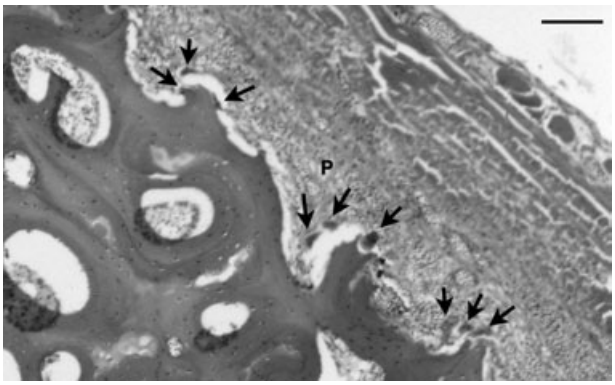

Figure 14. Irregular resorptive surface with large erosion bays lined by numerous osteoclasts (arrows), seen in transverse section (DMNH 83592, tibiotarsus section a). P, periosteum. Scale bar = 92 μm.

Although the adult size range is attained by late June or early July, approximately 2 months posthatching, the attainment of adult size did not correspond to the attainment of full skeletal maturity. This agrees with observations noted by previous authors for other avian taxa [Serjeantson (1998, 2002) for *Grus* and *Anser*, Mannermaa (2002) for *Cepphus*]. Although it is generally accepted that bone growth in *B. canadensis* is essentially complete by fledging (e.g. Owen, 1980), this generalization appears applicable to longitudinal growth only. The subadult age class is here established for hatching-year birds that have reached adult size ranges but are not yet fully skeletally mature. Subadult bones are characterized by texture types II–V, the temporal restriction of which suggests that these textures are outgrown by the end of the first autumn. Subadult shaft texture has at least some areas of penetrating porosity or well-defined longitudinally directed texture, but always lacks the striations seen in juveniles.

Adult birds are those that have attained both adult size and skeletal maturity. According to the texture distribution by date of death plots (Fig. 10), this seems to occur by December of the hatching year at approximately 7 months of age. Adult bones are characterized by texture types VI and VII, and may be described as grossly smooth elements completely lacking any penetrating porosity, although faint nonpenetrating longitudinal surface grooves are occasionally seen in some regions. Smooth in this case refers to a lack of porosity; transverse wrinkling and rugose textures do occur on adult bones. Given the general reduction in porosity and longitudinal textures through the subadult and into the adult ranges, it is possible that texture type VII (complete absence of any longitudinal texture) identifies older adults than type VI (co-occurrence of smooth areas and areas with faint longitudinal grooves). This cannot be confirmed, however, in the absence of absolute age data for these individuals.

Although the age classes defined here are not equivalent to those previously recognized for *B. canadensis* by Hanson (1965, 1967), they bear some similarity to ageing schemes utilized in the archaeozoological literature. Gotfredsen (1997) differentiated three age classes in several species of sea birds using a combination of surface porosity and epiphyseal fusion. Juveniles were identified by porous bone surfaces and unfused epiphyses, subadults by porous surfaces and partially fused epiphyses, and adults by nonporous surfaces and complete epiphyseal fusion. Gotfredsen (1997: Fig. 2) illustrated a series of juvenile gull humeri that appear to exhibit type 1 texture. Serjeantsen's (1998: figs 5–7) photographs of long bones from

immature *Grus* also show proximal striations suggestive of the type I textural pattern. This apparent presence of similar juvenile textures in gulls and cranes raises the possibility that the age and texture classes defined here for *B. canadensis* may be more broadly applicable to other avian taxa.

There was a close relationship between size-based maturity estimates and percentage maturity as determined by parsimony and cluster analyses for individuals over 35% mature (Fig. 4). There was less correspondence below 35% maturity. This was not surprising, as gosling growth rates are known to be highly variable depending on the quality and quantity of available food resources (Leafloor *et al*., 1998; Cooch *et al*., 1999). Both size-based and size-independent maturity estimates allowed recognition of the juvenile and adult age classes (Figs 8, 9). The subadult class was readily differentiated by relative maturity when either size-independent method was used (Fig. 9). Size-based maturity estimates, although not completely invalid, were of somewhat limited utility. The subadult class could not be distinguished by size-based maturity estimates alone, although it could be recognized by its temporal distribution on the texture type vs. date of death plots (Fig. 10).

Inter-element variation

The tendency for immature texture types to persist longer on the humerus than on the femur and/or tibiotarsus of a given individual was not unexpected. This pattern of differential maturity has been previously noted in *Anser* (Serjeantson, 2002). In *B. canadensis*, as in other geese, the hindlimb develops adult form and function earlier than the wing (Owen, 1980; Sedinger, 1986). Sedinger (1986) reported that leg muscle weights in *B. c. minima* goslings rapidly increase until 30–35 days posthatching, whereas pectoral muscles do not show their most rapid growth until shortly before fledging (more than 40 days posthatching). It should be noted that *B. c. minima* is the smallest subspecies of *B. canadensis*, and that fledging in the larger subspecies occurs relatively later, usually 8–9 weeks posthatching (Elder in Palmer, 1976).

Potentially more important than the variation in textural type, however, is the fact that femur, tibiotarsus, and humerus from the same individual did not always fall into the same age class. In 15% of the individuals examined (12 birds), at least one element fell into a different age class than the others (Table 9). This raises a crucial question: how does one assign an individual to an age class if more than one age class is represented in the skeleton? If multiple elements are known, it seems prudent to take the middle ground and define the individual as a subadult if any one element is assigned subadult status (that is, displays any one of texture types II–V). When working with isolated elements, however, the situation becomes more problematic. An individual with a subadult humerus and an adult femur would be classed as an adult if only the femur were known. In contrast, an individual might be classified as a juvenile on the basis of the humerus, when both hindlimb elements might have possessed subadult features. In the absence of multiple bones from the same individual, this problem is unavoidable. Therefore, when working with isolated bones, it is more appropriate to refer to the juvenile, subadult, and adult status of elements, rather than attempting to infer the skeletal maturity of the individual as a whole.

Table 9. Individuals with elements representing more than one age class. Roman numerals indicate texture types

Individual	Femur	Tibiotarsus	Humerus
DMNH 76885	Subadult II	Juvenile I	Juvenile I
DMNH 82727	Subadult II	Juvenile I	Juvenile I
DMNH 82247	Subadult II	Subadult II	Juvenile I
DMNH 81353	Subadult II	Subadult III	Juvenile I
DMNH 79340	Subadult IV	Adult VI	Adult VI
DMNH 82732	Subadult V	Adult VI	Subadult IV
DMNH 82729	Subadult V	Adult VI	Adult VI
DMNH 82271	Adult VI	Subadult III	Subadult III
DMNH 82228	Adult VI	Subadult III	Subadult IV
DMNH 82731	Adult VI	Subadult III	Subadult IV
DMNH 77108	Adult VI	Subadult IV	Subadult IV
DMNH 78500	Adult VI	Subadult V	Subadult IV

Ontogenetic texture change as a product of growth regime

Enlow & Brown (1958) and Cormack (1987) described a process by which subperiosteal vasculature is incorporated into the bone cortex during growth. The surface of a growing bone exhibits a series of subparallel ridges and furrows, and blood vessels running within the furrows are eventually incorporated within the bone matrix as a result of appositional growth along the ridges. New bone deposited within the channels thus formed eventually results in the formation of primary osteons (Cormack, 1987; Castanet *et al*., 2000; de Margerie *et al*., 2002). It is the ridge-and-furrow system that is manifest grossly as parallel striations on the bone surface. Not surprisingly, these striations and the longitudinal channel network associated with them are most commonly found on the proximal and distal thirds of the bone shaft, the regions of most active growth. In regions closer to the midshaft, a more fibrous or porous texture is present. Like the striations, these textures are associated with a highly

vascularized cortex, but the primary orientation of channels is oblique rather than strictly longitudinal. In mature bone, as growth slows and ceases, subperiosteal bone deposition and incorporation of new periosteal vasculature assumes a much-reduced importance; this accounts for a general reduction and loss of striated and other porous textural types.

Extant birds exhibit determinate growth; individuals undergo an initial uninterrupted period of rapid active growth, which dramatically slows to near cessation when the adult size is attained and the skeleton reaches maturity (Bennett, 1993; Chinsamy & Dodson, 1995; Chinsamy, Chiappe & Dodson, 1995). Growth after this point is minimal; although new bony material may be added during processes of secondary reconstruction, deposition is generally preceded by resorption of previously existing bone tissue (Cormack, 1987). In modern neognathous birds, the period of rapid growth is short; individuals reach skeletal maturity within one season. Palmer (1976) noted that *B. canadensis* goslings generally reach the adult size of their parents by 2 months of age.

As growth rates progressively decrease throughout ontogeny, the rate of osteogenesis and the type of bone produced likewise changes (Enlow & Brown, 1957; Chinsamy & Dodson, 1995; Chinsamy *et al*., 1995; Chinsamy, 1995a; Castanet *et al*., 1996, 2000; de Margerie *et al*., 2002, 2004). Observations of cortical bone in the auto-control sample agree with those of previous authors. The compact bone wall in immature birds consists of a single layer of highly vascularized fibrolamellar tissue; this coincides with the period of rapid growth to adult size. This central layer is covered periosteally and endosteally by circumferential lamellar bone tissue as growth slows and eventually ceases with the attainment of skeletal maturity. These internal and external circumferential lamellae are less densely vascularized than the immature fibrolamellar tissue (Meister, 1951; Enlow & Brown, 1957, 1958; Cormack, 1987; Chinsamy & Dodson, 1995; Chinsamy *et al*., 1995; Chinsamy, 1995a; Ponton *et al*., 2004).

This general growth pattern of modern birds is in many ways similar to that observed in pterodactyloid pterosaurs (Enlow & Brown, 1957, 1958; Bennett, 1993; de Ricqlès *et al*., 2000; Sayão, 2003), although not to the pattern seen in the smaller nonpterodactyloids (Padian *et al*., 2004). Among previous studies employing bone texture changes as ontogenetic indicators, Bennett (1993) provided the only detailed account relating macroscopic textures to underlying histological features. The entire bony cortex in actively growing immature pterodactyloids is characterized by fibrolamellar bone. Canals frequently penetrate the periosteal surface of the bone, accounting for its porous appearance. Bennett (1993) referred to these as vascular canals; however, as observed by Starck & Chinsamy (2002) and the present study, channels in the fibrolamellar bone of immature birds may also contain lymphatic vessels, nerves, and connective tissue such that the actual area occupied by vasculature is significantly less than the total channel diameter. It seems reasonable to assume that this was the case in pterosaurs as well. In adult pterodactyloids, as in adult birds, the subperiosteal cortical bone is composed of dense lamellar bone tissue, and adult bone therefore lacks the surface porosity found in subadults (Bennett, 1993; de Ricqlès *et al*., 2000). For the most part, the relationship between histology and bone surface texture in *B. canadensis* follows the pattern observed by Bennett (1993) in pterodactyloids. Bennett did not report a striated surface pattern; however, he also did not identify individuals younger than purported subadults based on their size. One important difference observed in the present study was that nonporous surface textures in *B. canadensis* were not always associated with lamellar bone. A grossly smooth texture may also be underlain by fibrolamellar bone if the number of channels penetrating the periosteal surface is suitably reduced.

Potential significance of subadult geese

Although most palaeontological and archaeozoological studies have been concerned with classifying skeletal material at the general immature vs. mature (juvenile vs. adult) level, there is a documented case in which clear recognition of a subadult age class may be of considerable significance. Serjeantson (2002) discussed the importance of the age distribution of goose remains for inferring the principle economic use of the birds. Where geese were kept primarily for their feathers, one would expect to see the remains dominated by adult individuals. Where the birds were raised primarily for meat, one would expect remains of three age classes: 12–16 weeks ('green geese'), 6–10 months ('stubble geese'), and adult birds of at least 5 years. The younger age classes represent birds raised for meat; the adult birds would have been breeding stock as well as a source of feathers.

The problem lies in recognizing the three classes from skeletal material. On the basis of observations of modern *Anser* skeletons, Serjeantson (2002) concluded that most birds would have been mature by 16 weeks of age. Therefore, all three stages would contain birds classified as adults by standard ageing schemes, and, with the exception of the youngest green geese, would be virtually indistinguishable in the zooarchaeological record.

If patterns of ontogenetic textural change in *Anser* are similar to those observed in *Branta*, the textural ageing scheme described here may help to resolve this

problem. Depending on the skeletal elements examined, birds from 3 to 4 months old (green geese) should exhibit texture types II–V. (Some would probably exhibit type I as well, but as type I seems broadly equivalent to a widely recognized juvenile condition, and type I bones tend to be smaller than adult size ranges, it is unlikely that these individuals would ever be mistaken for adults.) Birds from 6 to 10 months old (stubble geese) would be more difficult to distinguish, but might be expected to exhibit texture types IV and V. Recognition of the subadult age class (texture types II–V) would therefore help to distinguish both green and stubble geese from older adult birds. Separation of early (types II and III) and late (types IV and V) subadult textures might further distinguish green from stubble geese, although, due to variation in the timing of texture changes on different skeletal elements, assignments would probably be less reliable for late-maturing bones such as humeri.

CONCLUSIONS

A consistent relationship between bone surface textures and skeletal maturity was seen in *B. canadensis*. Seven distinct surface textural types were recognizable in the femur, tibiotarsus, and humerus. On the basis of the distributions of these types, three stages in relative skeletal maturity may be defined – juvenile, subadult, and adult. Juvenile bones are characterized by a fibrous or porous shaft surface, with parallel longitudinal striations in proximal and/or distal regions. Subadult bones are characterized by penetrating porosity or well-defined longitudinally directed texture in at least some shaft areas, and a lack of striations. Adult texture lacks all penetrating surface textures, although faint longitudinal surface grooves or dimples without associated pores may occur in isolated patches. The statistical analysis revealed that the relationship between bone texture and ontogenetic stage was robust, despite the possible presence of up to four different subspecies within the study sample. This has positive implications for the use of textural ageing in an archaeological and palaeontological context, where taxonomic resolution at the subspecies or even the species level may be uncertain.

Juvenile and subadult textures in *B. canadensis* are restricted to bones of hatching-year individuals, and appear to be outgrown by the end of an individual's first autumn. Subadult texture is further confined to bones of adult size ranges, although these bones have not yet reached full maturity. Subadult textures may be particularly useful for identifying older immature birds that would be lumped with adults by other ageing criteria; this would be particularly useful in zooarchaeological studies of domestic birds. Different elements from the same individual do not always exhibit the same texture type, and in some cases may not even fall within the same maturity level. In particular, there is a tendency for the maturity of the humerus to lag behind that of hindlimb elements. When using textural characters as ontogenetic indicators, it is therefore better to refer to the maturity levels of elements rather than individuals, especially in cases where only one element is known.

The juvenile and adult age classes may be readily distinguished by either size-based or size-independent estimates of skeletal maturity. A size-independent maturity estimate is needed to differentiate the subadult class from the adults in the absence of date of death data. The parsimony-based and cluster-based maturity estimates succeed equally well in this regard. Size-based maturity estimates are by no means invalid; however, they may be of limited utility, depending on the growth pattern of the taxon in question. It is therefore desirable to supplement size-based estimates with additional data (in this case, date of death) and/or size-independent maturity estimates whenever possible.

The histological analysis revealed that surface features associated with penetrating porosity (striated, fibrous and porous textures) result from the intersection of channels in underlying fibrolamellar bone with the bone surface. These channels are conduits for blood and lymphatic vessels; they also contain varying amounts of connective tissue. Thus, the presence of a striated, fibrous or porous surface texture is definitively associated with highly vascular, actively growing bone. The specific textural pattern is related to the orientation of the channels; with striations occurring where channels are primarily longitudinal, and fibrous and porous textures associated with more oblique channel orientations. Nonporous textures are either underlain by lamellar bone, or by fibrolamellar bone with little to no surface exposure of the channels.

The regular patterns of bone textural change seen in *B. canadensis* are therefore directly related to the determinate growth pattern characteristic of extant birds. Striated, fibrous, and porous textures are associated with the uninterrupted deposition of highly vascular fibrolamellar bone formed during rapid growth to adult size during early ontogeny. As growth slows, fewer channels pierce the bone surface, and grossly nonporous surfaces appear. A completely nonporous surface is seen in adult bones where the deposition of fibrolamellar bone has ceased, and circumferential deposits of lamellar bone underlie the periosteal surface.

Given that this growth regime is common to modern birds, it is reasonable to assume that ontogenetic patterns of bone texture change in other species may be similar to those observed in *B. canadensis*. Illustra-

tions of juvenile gull (Gotfredsen, 1997) and crane (Serjeantson, 1998) bones from archaeological sites offer further support for this assumption. Similarly, bone texture changes are probably reliable indicators of relative skeletal maturity in extinct taxa with similar growth regimes (e.g. many fossil birds and pterodactyloid pterosaurs). This strong relationship between textural changes and growth regime, however, suggests that the results reported here will not be universally applicable. Preliminary findings reported for the American alligator *Alligator mississippiensis* (Tumarkin-Deratzian, 2002) suggest that the textural ageing method may not be useful for taxa with indeterminate and/or cyclical growth patterns, such as those of crocodylians. All this considered, the applicability of the method to most non-avian archosaurs will need to be evaluated on a case-by-case basis, and ideally only in taxa for which some prior understanding of the growth regime is possible.

ACKNOWLEDGEMENTS

The following individuals and institutions granted access to specimens within their care, and provided assistance in the preparation of samples for the autocontrol study: Gene Hess, Barbara Luff, Leslie Skibinski, and Jean Woods (DMNH); Erica Miller and Sallie Welte (TSBR). Thin sections were prepared by the University of Pennsylvania School of Veterinary Medicine Histopathology Laboratory; special thanks are given to Juliana Burns and Linden Craig. David Deratzian provided technical assistance with photographic images. Anusuya Chinsamy-Turan, Art Johnson, and Hermann Pfefferkorn reviewed earlier drafts of this manuscript. Barbara Grandstaff provided much helpful discussion. Portions of this work were supported by the Geological Society of America, the Paleontological Society, the University of Pennsylvania Summer Stipends in Paleontology program, and a National Science Foundation Graduate Research Fellowship to Allison R. Tumarkin-Deratzian.

REFERENCES

Bellrose FC. 1980. *Ducks, geese and swans of North America*, 3rd edn. Harrisburg, Pennsylvania: Stackpole Books.

Benecke N. 1993. On the utilization of the domestic fowl in central Europe from the Iron Age up to the Middle Ages. *Archaeofauna* **2:** 21–31.

Bennett SC. 1993. The ontogeny of *Pteranodon* and other pterosaurs. *Paleobiology* **19:** 92–106.

Brill K, Carpenter K. 2001. A baby ornithopod from the Morrison Formation of Garden Park, Colorado. In: Tanke DH, Carpenter K, eds. *Mesozoic vertebrate life*. Bloomington: Indiana University Press, 197–205.

Brinkman D. 1988. Size-independent criteria for estimating relative age in *Ophiacodon* and *Dimetrodon* (Reptilia, Pelycosauria) from the Admiral and Lower Belle Plains Formations of west-central Texas. *Journal of Vertebrate Paleontology* **8:** 172–180.

Brochu CA. 1996. Closure of neurocentral sutures during crocodilian ontogeny: implications for maturity assessment in fossil archosaurs. *Journal of Vertebrate Paleontology.* **16:** 49–62.

Callison G, Quimby HM. 1984. Tiny dinosaurs: are they fully grown? *Journal of Vertebrate Paleontology* **3:** 200–209.

Carey G. 1982. Ageing and sexing domestic bird bones from some Late Medieval deposits at Baynard's Castle, City of London. In: Wilson B, Grigson C, Payne S, eds. *Ageing and sexing animal bones from archaeological sites*, Vol. 109. Oxford: BAR British Series, 263–268.

Carr TD. 1999. Craniofacial ontogeny in Tyrannosauridae (Dinosauria, Coelurosauria). *Journal of Vertebrate Paleontology* **19:** 497–520.

Castanet J, Curry-Rogers K, Cubo J, Boisard JJ. 2000. Periosteal bone growth rates in extant ratites (ostrich and emu). Implications for assessing growth in dinosaurs. *Comptes Rendus de l'Académie des Sciences Paris, Sciences de la Vie* **323:** 543–550.

Castanet J, Grandin A, Abourachid A, de Ricqlès A. 1996. Expression de la dynamique de croissance dans la structure de l'os périostique chez *Anas platyrhynchos*. *Comptes Rendus d'Académie des Sciences, Paris, Sciences de la Vie* **319:** 301–308.

Chinsamy A. 1990. Physiological implications of the bone histology of *Syntarsus rhodesiensis* (Saurischia: Theropoda). *Palaeontologia Africana* **27:** 77–82.

Chinsamy A. 1993. Image analysis and the physiological implications of the vascularisation of femora in archosaurs. *Modern Geology* **19:** 101–108.

Chinsamy A. 1995a. Histological perspectives on growth in the birds *Struthio camelus* and *Sagittarius serpentarius*. *Courier Forschungsinstitut Senckenberg* **181:** 317–323.

Chinsamy A. 1995b. Ontogenetic changes in the bone histology of the Late Jurassic ornithopod *Dryosaurus lettowvorbecki*. *Journal of Vertebrate Paleontology* **15:** 96–104.

Chinsamy A, Chiappe LM, Dodson P. 1995. Mesozoic avian bone microstructure: physiological implications. *Paleobiology* **21:** 561–574.

Chinsamy A, Dodson P. 1995. Inside a dinosaur bone. *American Scientist* **83:** 174–180.

Chinsamy A, Elzanowski A. 2001. Evolution of growth pattern in birds. *Nature* **412:** 402–403.

Cohen A, Serjeantson D. 1996. *A manual for the identification of bird bones from archaeological sites*, revised edn. London: Archetype Publications.

Cooch EG, Dzubin A, Rockwell RF. 1999. Using body size to estimate gosling age. *Journal of Field Ornithology* **70:** 214–229.

Cormack DH. 1987. *Ham's history*, 9th edn. Philadelphia: J. B. Lippincott.

Cracraft J. 1986. The origin and early diversification of birds. *Paleobiology* **12:** 383–399.

Craighead JJ, Stockstad DS. 1964. Breeding age of Canada geese. *Journal of Wildlife Management* **28:** 57–64.

Curry KA. 1999. Ontogenetic histology of *Apatosaurus* (Dinosauria: Sauropoda): new insights on growth rates and longevity. *Journal of Vertebrate Paleontology* **19:** 654–665.

Delacour J. 1951. Preliminary note on the taxonomy of Canada geese, *Branta canadensis*. *American Museum Novitates* **1537:** 1–10.

Delacour J. 1954. *The waterfowl of the world*, Vol. 1. London: Country Life.

Dodson P. 1975. Taxonomic implications of relative growth in lambeosaurine hadrosaurs. *Systematic Zoology* **24:** 37–54.

Enlow DH, Brown SO. 1957. A comparative histological study of fossil and recent bone tissues. Part II. *Texas Journal of Science* **9:** 186–214.

Enlow DH, Brown SO. 1958. A comparative histological study of fossil and recent bone tissues. Part III. *Texas Journal of Science* **10:** 187–230.

Gilbert BM, Martin LD, Savage HG. 1996. *Avian osteology*, 2nd edn. Columbia: Missouri Archaeological Society.

Gotfredsen AB. 1997. Sea bird exploitation on coastal Inuit sites, West and Southeast Greenland. *International Journal of Osteoarchaeology* **7:** 271–286.

Gotfredsen AB. 2002. Former occurrences of geese (genera *Anser* and *Branta*) in ancient West Greenland: morphological and biometric approaches. *Acta Zoologica Cracoviensia* **45:** 179–204.

Hanson HC. 1965. *The giant Canada goose*. Carbondale: Southern Illinois University Press.

Hanson HC. 1967. *Characters of age, sex, and sexual maturity in Canada geese*. Biological Notes no. 49. Urbana: Natural History Survey Division, State of Illinois Department of Registration and Education.

Hartman FE, Dunn JP. 1998. The Canada goose in Pennsylvania: from none to too many. In: Rusch DH, Samuel MD, Humburg DD, Sullivan BD, eds. *Biology and management of Canada geese. Proceedings of the International Canada Goose Symposium.* Milwaukee, Wisconsin, 477.

Hess GK, West RL, Barnhill MV III, Fleming LM. 2000. *Birds of Delaware*. Pittsburgh: University of Pittsburgh Press.

Horner JR, Currie PJ. 1994. Embryonic and neonatal morphology and ontogeny of a new species of *Hypacrosaurus* (Ornithischia: Lambeosauridae) from Montana and Alberta. In: Carpenter K, Hirsch KF, Horner JR, eds. *Dinosaur eggs and babies*. Cambridge: Cambridge University Press, 312–336.

Horner JR, de Ricqlès A, Padian K. 1999. Variation in dinosaur skeletochronology indicators: implications for age assessment and physiology. *Paleobiology* **25:** 295–304.

Horner JR, de Ricqlès A, Padian K. 2000. Long bone histology of the hadrosaurid dinosaur *Maiasaura peeblesorum*: growth dynamics and physiology based on an ontogenetic series of skeletal elements. *Journal of Vertebrate Paleontology* **20:** 115–129.

Hutton MacDonald R, MacDonald KC, Ryan K. 1993. Domestic geese from Medieval Dublin. *Archaeofauna* **2:** 205–218.

Jacobs LL, Winkler DA, Murry PA, Maurice JM. 1994. A nodosaurid scuteling from the Texas shore of the Western Interior Seaway. In: Carpenter K, Hirsch KF, Horner JR, eds. *Dinosaur eggs and babies*. Cambridge: Cambridge University Press, 337–346.

Johnsgard PA. 1975. *Waterfowl of North America*. Bloomington: Indiana University Press.

Johnson R. 1977. Size independent criteria for estimating relative age and the relationships among growth parameters in a group of fossil reptiles (Reptilia: Ichthyosauria). *Canadian Journal of Earth Sciences* **14:** 1916–1924.

Johnson FA, Castelli PM. 1998. Demographics of 'resident' Canada geese in the Atlantic Flyway. In: Rusch DH, Samuel MD, Humburg DD, Sullivan BD, eds. *Biology and management of Canada geese. Proceedings of the International Canada Goose Symposium.* Milwaukee, Wisconsin, 127–133.

Leafloor JO, Ankney CD, Rusch DH. 1998. Environmental effects on body size of Canada geese. *Auk* **115:** 26–33.

Mannermaa K. 2002. Bird bones from Jettböle I, a site in the Neolithic Åland archipelago in the northern Baltic. *Acta Zoologica Cracoviensia* **45:** 85–98.

de Margerie E, Cubo J, Castanet J. 2002. Bone typology and growth rate: testing and quantifying 'Amprino's rule' in the mallard (*Anas platyrhynchos*). *Comptes Rendus Biologies* **325:** 221–230.

de Margerie E, Robin J-P, Verrier D, Cubo J, Groscolas R, Castanet J. 2004. Assessing a relationship between bone microstructure and growth rate: a fluorescent labelling study in the king penguin chick (*Aptenodytes patagonicus*). *Journal of Experimental Biology* **207:** 869–879.

Meanley B. 1982. *Waterfowl of the Chesapeake Bay country*. Centreville, Maryland: Tidewater Publishers.

Meister W. 1951. Changes in histological structure of the long bones of birds during the molt. *Anatomical Record* **111:** 1–21.

Nelson HK, Oetting RB. 1998. Giant Canada goose flocks in the United States. In: Rusch DH, Samuel MD, Humburg DD, Sullivan BD, eds. *Biology and management of Canada geese. Proceedings of the International Canada Goose Symposium.* Milwaukee, Wisconsin, 483–495.

Owen M. 1980. *Wild geese of the world: their life history and ecology*. London: B. T. Batsford.

Padian K, Horner JR, de Ricqlès A. 2004. Growth in small dinosaurs and pterosaurs: the evolution of archosaurian growth strategies. *Journal of Vertebrate Paleontology* **24:** 555–571.

Palmer RS. 1976. *Handbook of North American birds*, Vol. 2. New Haven: Yale University Press.

Ponton F, Elzanowski A, Castanet J, Chinsamy A, de Margerie E, de Ricqlès A, Cubo J. 2004. Variation of the outer circumferential layer in the limb bones of birds. *Acta Ornithologica* **39:** 137–140.

de Ricqlès AJ. 1974. Evolution of endothermy: histological evidence. *Evolutionary Theory* **1:** 51–80.

de Ricqlès AJ. 1976. On bone histology of fossil and living reptiles, with comments on its functional and evolutionary significance. In: Bellairs A, Cox CB, eds. *Morphology and biology of reptiles*. New York: Academic Press, 123–151.

de Ricqlès AJ, Padian K, Horner JR. 1993. Paleohistology of pterosaur bones. *Journal of Vertebrate Paleontology* **13:** 54A.

de Ricqlès AJ, Padian K, Horner JR, Francillon-Vieillot H. 2000. Palaeohistology of the bones of pterosaurs (Reptilia: Archosauria): anatomy, ontogeny and biomechanical implications. *Zoological Journal of the Linnean Society* **129:** 349–385.

de Ricqlès AJ, Padian K, Horner JR, Lamm E-T, Myhrvold N. 2003. Osteohistology of *Confuciusornis sanctus* (Theropoda: Aves). *Journal of Vertebrate Paleontology* **23:** 373–386.

Ryan MJ, Russell AP, Eberth DA, Currie PJ. 2001. The taphonomy of a *Centrosaurus* (Ornithischia: Ceratopsidae) bone bed from the Dinosaur Park Formation (Upper Campanian), Alberta, Canada, with comments on cranial ontogeny. *Palaios* **16:** 482–506.

Sadler P. 1991. The use of tarsometatarsi in sexing and ageing domestic fowl (*Gallus gallus* L.), and recognising five toed breeds in archaeological material. *Circaea* **8:** 41–48.

Sampson SD, Ryan MJ, Tanke DH. 1997. Craniofacial ontogeny in centrosaurine dinosaurs (Ornithischia: Ceratopsidae): taxonomic and behavioural implications. *Zoological Journal of the Linnean Society* **121:** 293–337.

Sander PM. 2000. Longbone histology of the Tendaguru sauropods: implications for growth and biology. *Paleobiology* **26:** 466–488.

Sanz JL, Chiappe LM, Pérez-Moreno BP, Moratalla JJ, Hernández-Carrasquilla F, Buscalioni AD, Ortega F, Poyato-Ariza FJ, Rasskin-Gutman D, Martinez-Delclòs X. 1997. A nestling bird from the Lower Cretaceous of Spain: implications for avian skull and neck evolution. *Science* **276:** 1543–1546.

Sayão JM. 2003. Histovariability in bones of two pterodactyloid pterosaurs from the Santana Formation, Araripe Basin, Brazil. Preliminary results. In: Buffetaut E, Mazin J-M, eds. *Evolution and palaeobiology of pterosaurs.* Special Publication 217. London: Geological Society, 335–342.

Sedinger JS. 1986. Growth and development of Canada goose goslings. *Condor* **88:** 169–180.

Serjeantson D. 1998. Birds: a seasonal resource. *Environmental Archaeology* **3:** 23–33.

Serjeantson D. 2002. Goose husbandry in Medieval England, and the problem of ageing goose bones. *Acta Zoologica Cracoviensia* **45:** 39–54.

Sheaffer SE, Malecki RA. 1998. Status of Atlantic Flyway resident nesting Canada geese. In: Rusch DH, Samuel MD, Humburg DD, Sullivan BD, eds. *Biology and management of Canada geese. Proceedings of the International Canada Goose Symposium.* Milwaukee, Wisconsin, 29–34.

Starck JM, Chinsamy A. 2002. Bone microstructure and developmental plasticity in birds and other dinosaurs. *Journal of Morphology* **254:** 232–246.

Stotts VD. 1983. *Canada goose management plan for the Atlantic Flyway, 1983–95: Part II – history and current status.* Atlantic Waterfowl Council.

Swofford DL. 1999. *PAUP* phylogenetic analysis using parsimony*, *Version* 4. Sunderland, Massachusetts: Sinauer Associates.

Tumarkin-Deratzian AR. 2002. Is bone surface texture an indicator of skeletal maturity in *Alligator mississippiensis*? *Proceedings of the 16th Working Meeting of the Crocodile Specialist Group*. Gland, Switzerland and Cambridge, UK: IUCN – the World Conservation Union, 141–151.

Varricchio DJ. 1993. Bone microstructure of the Upper Cretaceous theropod dinosaur *Troodon formosus*. *Journal of Vertebrate Paleontology* **13:** 99–104.

APPENDIX 1

TOTAL CHARACTER LIST FOR SIZE-INDEPENDENT MATURITY ESTIMATES

FEMUR

1. Bony femoral head: (0) absent; (1) present; (2) completely ossified.
2. Bony greater trochanter: (0) absent; (1) present; (2) completely ossified.
3. Bony distal condyles: (0) absent; (1) present; (2) completely ossified.
4. Cranial intermuscular line: (0) absent; (1) present.
5. Scar for M. tibialis cranialis: (0) absent; (1) present.
6. Scar for M. obturator externus: (0) absent; (1) present.
7. Caudal intermuscular line: (0) absent; (1) present.
8. Scar for M. puboischiofemoralis: (0) absent; (1) present.
9. Lateral tubercle for M. gastrocnemius: (0) absent; (1) present.
10. Medial scar for Mm. flexor perforati II and IV: (0) absent; (1) present.
11. Crista tibiofibularis: (0) absent; (1) present.
12. Scar for M. obturator internus: (0) absent; (1) present.
13. Lateral scar for M. iliotrochantericus caudalis: (0) absent; (1) present.
14. Scar for M. ischiofemoralis: (0) absent; (1) present.
15. Lateral scar for M. iliotrochantericus cranialis and medius: (0) absent; (1) present.
16. Scar for M. flexor perforans and perforatus II: (0) absent; (1) present.
17. Scar for M. flexor perforans and perforatus III: (0) absent; (1) present.
18. Lateral collateral ligament impression: (0) absent; (1) present.

TIBIOTARSUS

1. Bony proximal end: (0) absent; (1) present; (2) completely ossified.
2. Fusion of proximal end: (0) entire suture visible; (1) suture visible medially; (2) suture obliterated.

3. Bony distal condyles: (0) absent; (1) present; (2) completely ossified.
4. Popliteal tuberosities: (0) absent; (1) present.
5. Crista fibularis: (0) absent; (1) present.
6. Tubercle for Mm. peroneus longus and brevis retinaculum: (0) absent; (1) present.
7. Cranial cnemial crest: (0) absent; (1) present.
8. Lateral cnemial crest: (0) absent; (1) present.
9. Proximal scars for M. extensor digitorum longus: (0) absent; (1) present.
10. Extensor sulcus: (0) absent; (1) present.
11. Supratendinal bridge: (0) absent; (1) present.
12. Scar for M. femorotibialis externus: (0) absent; (1) present.
13. Peroneal sulcus: (0) absent; (1) present.
14. Scar for M. femorotibialis internus: (0) absent; (1) present.
15. Complex of scars for M. gastrocnemius pars medialis, M. plantaris, and Mm. flexores cruri lateralis and medialis: (0) absent; (1) present.
16. Distinct scars for M. plantaris and Mm. flexores cruri lateralis and medialis: (0) absent; (1) present.
17. Distinct scar for M. gastrocnemius pars medialis: (0) absent; (1) present.

HUMERUS

1. Bony humeral head: (0) absent; (1) present; (2) completely ossified.
2. Bony deltopectoral crest: (0) absent; (1) present.
3. Bony distal condyles: (0) absent; (1) present; (2) completely ossified.
4. Scar for M. pectoralis: (0) absent; (1) present.
5. Capital notch: (0) absent; (1) present.
6. Pneumatic foramen: (0) absent; (1) present.
7. Groove for M. scapulotriceps tendon: (0) absent; (1) present.
8. Groove for M. humerotriceps tendon: (0) absent; (1) present.
9. Dorsal tubercle: (0) absent; (1) present.
10. Transverse ligamental groove: (0) absent; (1) present.
11. Impression of M. coracobrachialis: (0) absent; (1) present.
12. Bicipital crest: (0) absent; (1) present.
13. Fossa for M. brachialis: (0) absent; (1) present.
14. Linea M. latissimus dorsi: (0) absent; (1) present.

APPENDIX 2

Bone landmark character matrices for size-independent analyses. The character numbers and codes correspond to descriptions in Appendix 1. ? indicates missing data. Only those specimens marked with an asterisk were used in the parsimony analyses. DMNH 82688 was not used in the cluster analyses

Specimen number	Character number																	
	1	2	3	4	5	6	7	8	9	10	11	12	13	14	15	16	17	18
Femur																		
*Outgroup	0	0	0	0	0	0	0	0	0	0	0	0	0	0	0	0	0	0
*DMNH 35657	2	2	2	1	1	1	1	1	1	1	1	1	1	1	1	1	1	1
DMNH 73095	2	2	2	1	1	1	1	1	1	1	1	1	1	1	1	1	1	1
DMNH 76523	2	2	2	1	1	1	1	1	1	1	1	1	1	1	1	1	1	1
DMNH 76661	2	2	2	1	1	1	1	1	1	1	1	1	1	1	1	1	1	1
*DMNH 76826	1	1	1	1	1	1	1	1	1	1	1	1	1	1	1	1	1	1
DMNH 76856	2	2	2	1	1	1	1	1	1	1	1	1	1	1	1	1	1	1
*DMNH 76885	1	1	1	1	1	0	1	1	1	0	1	0	1	1	1	0	1	1
DMNH 77084	2	2	2	1	1	1	1	1	1	1	1	1	1	1	1	1	1	1
DMNH 77107	2	2	2	1	1	1	1	1	1	1	1	1	1	1	1	1	1	1
DMNH 77108	2	2	2	1	1	1	1	1	1	1	1	1	1	1	1	1	1	1
DMNH 77170	2	2	2	1	1	1	1	1	1	1	1	1	1	1	1	1	1	1
DMNH 77234	2	2	2	1	1	1	1	1	1	1	1	1	1	1	1	1	1	1
DMNH 77256	2	2	2	1	1	1	1	1	1	1	1	1	1	1	1	1	1	1
DMNH 77273	2	2	2	1	1	1	1	1	1	1	1	1	1	1	1	1	1	1
DMNH 77287	2	2	2	1	1	1	1	1	1	1	1	1	1	1	1	1	1	1
DMNH 77371	2	2	2	1	1	1	1	1	1	1	1	1	1	1	1	1	1	1
DMNH 77472	2	2	2	1	1	1	1	1	1	1	1	1	1	1	1	1	1	1
DMNH 77751	2	2	2	1	1	1	1	1	1	1	1	1	1	1	1	1	1	1
DMNH 77767	2	2	2	1	1	1	1	1	1	1	1	1	1	1	1	1	1	1
*DMNH 77823	1	2	2	1	1	1	1	1	1	1	1	1	1	1	1	1	1	1
DMNH 78063	2	2	2	1	1	1	1	1	1	1	1	1	1	1	1	1	1	1
DMNH 78064	2	2	2	1	1	1	1	1	1	1	1	1	1	1	1	1	1	1
DMNH 78271	2	2	2	1	1	1	1	1	1	1	1	1	1	1	1	1	1	1
DMNH 78408	2	2	2	1	1	1	1	1	1	1	1	1	1	1	1	1	1	1
DMNH 78423	2	2	2	1	1	1	1	1	1	1	1	1	1	1	1	1	1	1
DMNH 78452	1	2	2	1	1	1	1	1	1	1	1	1	1	1	1	1	1	1
*DMNH 78500	2	2	2	1	1	1	1	1	1	0	1	1	1	1	1	1	1	1
DMNH 78603	1	1	1	1	1	1	1	1	1	1	1	1	1	1	1	1	1	1
DMNH 78628	2	2	2	1	1	1	1	1	1	1	1	1	1	1	1	1	1	1
DMNH 78681	2	2	2	1	1	1	1	1	1	1	1	1	1	1	1	1	1	1
DMNH 79337	2	2	2	1	1	1	1	1	1	1	1	1	1	1	1	1	1	1
DMNH 79340	2	2	2	1	1	1	1	1	1	1	1	1	1	1	1	1	1	1
DMNH 79386	2	2	2	1	1	1	1	1	1	1	1	1	1	1	1	1	1	1
DMNH 79452	2	2	2	1	1	1	1	1	1	1	1	1	1	1	1	1	1	1
DMNH 79989	2	2	2	1	1	1	1	1	1	1	1	1	1	1	1	1	1	1
DMNH 80059	2	2	2	1	1	1	1	1	1	1	1	1	1	1	1	1	1	1
DMNH 80060	2	2	2	1	1	1	1	1	1	1	1	1	1	1	1	1	1	1
DMNH 80062	2	2	2	1	1	1	1	1	1	1	1	1	1	1	1	1	1	1
DMNH 80066	2	2	2	1	1	1	1	1	1	1	1	1	1	1	1	1	1	1
DMNH 80067	2	2	2	1	1	1	1	1	1	1	1	1	1	1	1	1	1	1
DMNH 80068	2	2	2	1	1	1	1	1	1	1	1	1	1	1	1	1	1	1
DMNH 80472	1	2	2	1	1	1	1	1	1	1	1	1	1	1	1	1	1	1
DMNH 80844	2	2	2	1	1	1	1	1	1	1	1	1	1	1	1	1	1	1
DMNH 80847	2	2	2	1	1	1	1	1	1	1	1	1	1	1	1	1	1	1
DMNH 80850	2	2	2	1	1	1	1	1	1	1	1	1	1	1	1	1	1	1
DMNH 80851	2	2	2	1	1	1	1	1	1	1	1	1	1	1	1	1	1	1

APPENDIX 2 *Continued*

Specimen number	Character number																	
	1	2	3	4	5	6	7	8	9	10	11	12	13	14	15	16	17	18
*DMNH 81352	1	1	1	1	1	1	1	1	1	1	1	0	0	0	0	0	1	1
*DMNH 81353	1	1	1	1	1	1	1	1	1	1	1	1	0	0	0	0	1	1
DMNH 81354	2	2	2	1	1	1	1	1	1	1	1	1	1	1	1	1	1	1
*DMNH 81978	0	0	0	0	0	0	1	1	0	0	0	0	0	0	0	0	0	0
*DMNH 81979	0	0	0	0	0	0	0	1	1	0	0	0	0	0	0	0	0	0
DMNH 82228	2	2	2	1	1	1	1	1	1	1	1	1	1	1	1	1	1	1
*DMNH 82247	1	1	1	1	0	1	1	1	1	0	1	0	1	0	0	0	1	1
DMNH 82270	2	2	2	1	1	1	1	1	1	1	1	1	1	1	1	1	1	1
*DMNH 82271	1	1	1	1	1	0	1	1	1	1	1	1	1	1	1	1	1	1
DMNH 82543	2	2	2	1	1	1	1	1	1	1	1	1	1	1	1	1	1	1
*DMNH 82688	1	0	1	1	0	0	1	1	1	0	1	0	0	0	0	0	0	1
DMNH 82727	1	1	1	1	1	0	1	1	1	0	1	0	1	1	1	0	1	1
DMNH 82729	2	2	2	1	1	1	1	1	1	1	1	1	1	1	1	1	1	1
DMNH 82730	2	2	2	1	1	1	1	1	1	1	1	1	1	1	1	1	1	1
DMNH 82731	2	2	2	1	1	1	1	1	1	1	1	1	1	1	1	1	1	1
DMNH 82732	2	2	2	1	1	1	1	1	1	1	1	1	1	1	1	1	1	1
DMNH 82766	2	2	2	1	1	1	1	1	1	1	1	1	1	1	1	1	1	1
DMNH 82767	2	2	2	1	1	1	1	1	1	1	1	1	1	1	1	1	1	1
DMNH 82910	2	2	2	1	1	1	1	1	1	1	1	1	1	1	1	1	1	1
DMNH 82944	2	2	2	1	1	1	1	1	1	1	1	1	1	1	1	1	1	1
DMNH 83058	2	2	2	1	1	1	1	1	1	1	1	1	1	1	1	1	1	1
DMNH 83131	2	2	2	1	1	1	1	1	1	1	1	1	1	1	1	1	1	1
*DMNH 83585	0	0	1	0	0	0	1	1	0	0	0	0	0	0	0	0	0	0
*DMNH 83586	0	0	0	0	0	0	0	0	0	0	0	0	0	0	0	0	0	0
DMNH 83587	0	0	0	0	0	0	1	1	0	0	0	0	0	0	0	0	0	0
*DMNH 83588	1	0	1	1	0	0	1	1	1	0	0	0	0	0	0	0	0	0
*DMNH 83589	1	0	1	0	0	0	1	1	0	0	0	0	0	0	0	0	0	0
*DMNH 83590	1	0	1	1	0	0	1	1	1	0	1	0	0	0	0	0	0	0
DMNH 83591	2	2	2	1	1	1	1	1	1	1	1	1	1	1	1	1	1	1
*DMNH 83592	1	1	1	1	1	1	1	1	1	1	1	1	1	0	0	0	1	1
Tibiotarsus																		
*Outgroup	0	0	0	0	0	0	0	0	0	0	0	0	0	0	0	0	0	
*DMNH 35657	2	1	2	1	1	1	1	1	1	1	1	1	1	1	1	1	1	
DMNH 73061	2	1	2	1	1	1	1	1	1	1	1	1	1	1	1	1	1	
DMNH 73095	2	1	2	1	1	1	1	1	1	1	1	1	1	1	1	1	1	
*DMNH 76260	2	1	2	1	1	1	1	1	1	1	1	1	1	1	1	1	0	
DMNH 76661	2	1	2	1	1	1	1	1	1	1	1	1	1	1	1	1	1	
*DMNH 76826	1	?	1	0	1	1	1	1	1	1	1	1	1	1	1	1	0	
*DMNH 76885	1	0	1	0	1	1	1	1	1	1	1	1	1	1	1	0	0	
DMNH 77084	2	1	2	1	1	1	1	1	1	1	1	1	1	1	1	1	1	
*DMNH 77107	2	?	2	1	1	1	1	1	1	1	1	1	1	1	1	1	1	
*DMNH 77108	1	1	1	1	1	1	1	1	1	1	1	1	0	1	1	1	1	
DMNH 77170	2	1	2	1	1	1	1	1	1	1	1	1	1	1	1	1	1	
DMNH 77234	2	1	2	1	1	1	1	1	1	1	1	1	1	1	1	1	1	
DMNH 77256	2	1	2	1	1	1	1	1	1	1	1	1	1	1	1	1	1	
DMNH 77273	2	1	2	1	1	1	1	1	1	1	1	1	1	1	1	1	1	
DMNH 77287	1	1	1	1	1	1	1	1	1	1	1	1	1	1	1	1	1	
DMNH 77371	2	1	2	1	1	1	1	1	1	1	1	1	1	1	1	1	1	
DMNH 77472	2	1	2	1	1	1	1	1	1	1	1	1	1	1	1	1	1	
DMNH 77751	2	1	2	1	1	1	1	1	1	1	1	1	1	1	1	1	1	
DMNH 77767	2	1	2	1	1	1	1	1	1	1	1	1	1	1	1	1	1	
*DMNH 77823	1	1	0	1	1	1	1	1	1	1	1	1	1	1	1	0	0	

APPENDIX 2 *Continued*

Specimen number	Character number																	
	1	2	3	4	5	6	7	8	9	10	11	12	13	14	15	16	17	18
DMNH 78063	2	1	2	1	1	1	1	1	1	1	1	1	1	1	1	1	1	
DMNH 78064	2	1	2	1	1	1	1	1	1	1	1	1	1	1	1	1	1	
DMNH 78271	2	1	2	1	1	1	1	1	1	1	1	1	1	1	1	1	1	
DMNH 78408	2	1	2	1	1	1	1	1	1	1	1	1	1	1	1	1	1	
DMNH 78423	2	1	2	1	1	1	1	1	1	1	1	1	1	1	1	1	1	
*DMNH 78452	1	0	1	0	1	1	1	1	1	1	1	1	1	1	1	1	1	
DMNH 78500	2	?	2	1	1	1	1	1	1	1	1	1	1	1	1	1	1	
*DMNH 78603	1	1	1	1	1	1	1	1	1	1	1	1	1	1	1	0	0	
*DMNH 78628	2	1	1	1	1	1	1	1	1	1	1	1	1	1	1	1	0	
DMNH 78681	2	1	2	1	1	1	1	1	1	1	1	1	1	1	1	1	1	
DMNH 79337	2	1	2	1	1	1	1	1	1	1	1	1	1	1	1	1	1	
DMNH 79340	2	1	2	1	1	1	1	1	1	1	1	1	1	1	1	1	1	
DMNH 79386	2	?	2	1	1	1	1	1	1	1	1	1	1	1	1	1	1	
DMNH 79452	2	1	2	1	1	1	1	1	1	1	1	1	1	1	1	1	1	
DMNH 80059	2	?	2	1	1	1	1	1	1	1	1	1	1	1	1	1	1	
DMNH 80060	2	1	2	1	1	1	1	1	1	1	1	1	1	1	1	1	1	
DMNH 80062	2	1	2	1	1	1	1	1	1	1	1	1	1	1	1	1	1	
DMNH 80066	2	1	2	1	1	1	1	1	1	1	1	1	1	1	1	1	1	
DMNH 80067	2	1	2	1	1	1	1	1	1	1	1	1	1	1	1	1	1	
*DMNH 80068	2	2	2	1	1	1	1	1	1	1	1	1	1	1	1	1	1	
DMNH 80472	2	1	2	1	1	1	1	1	1	1	1	1	1	1	1	1	1	
DMNH 80844	2	1	2	1	1	1	1	1	1	1	1	1	1	1	1	1	1	
DMNH 80846	2	1	2	1	1	1	1	1	1	1	1	1	1	1	1	1	1	
*DMNH 80847	1	1	2	1	1	1	1	1	1	1	1	1	1	1	1	1	1	
DMNH 80850	2	1	2	1	1	1	1	1	1	1	1	1	1	1	1	1	1	
DMNH 80851	2	1	2	1	1	1	1	1	1	1	1	1	1	1	1	1	1	
*DMNH 81352	1	?	1	0	1	1	1	1	1	1	1	1	0	1	1	1	0	
*DMNH 81353	1	1	1	0	1	1	1	1	1	1	1	1	1	1	1	0	0	
DMNH 81354	2	1	2	1	1	1	1	1	1	1	1	1	1	1	1	1	1	
*DMNH 81978	0	0	0	0	0	0	0	0	0	1	0	0	0	0	0	0	0	
DMNH 81979	0	0	0	0	0	0	0	0	0	1	0	0	0	0	0	0	0	
*DMNH 82228	2	1	2	1	1	1	1	1	1	1	1	1	0	1	1	1	0	
DMNH 82247	1	1	1	0	1	1	1	1	1	1	1	1	1	1	1	0	0	
DMNH 82270	2	1	2	1	1	1	1	1	1	1	1	1	1	1	1	1	1	
*DMNH 82271	1	1	1	0	1	1	1	1	1	1	1	1	1	1	1	1	0	
DMNH 82543	2	1	2	1	1	1	1	1	1	1	1	1	1	1	1	1	1	
*DMNH 82688	0	0	1	0	1	1	0	0	0	0	?	0	?	0	0	0	0	
DMNH 82727	1	0	1	0	1	1	1	1	1	1	1	1	1	1	1	0	0	
DMNH 82729	2	1	2	1	1	1	1	1	1	1	1	1	1	1	1	1	1	
DMNH 82730	2	1	2	1	1	1	1	1	1	1	1	1	1	1	1	1	1	
DMNH 82731	2	1	2	1	1	1	1	1	1	1	1	1	1	1	1	1	1	
DMNH 82732	2	1	2	1	1	1	1	1	1	1	1	1	1	1	1	1	1	
*DMNH 82766	2	1	2	0	1	1	1	1	1	1	1	1	1	1	1	1	1	
DMNH 82767	2	1	2	1	1	1	1	1	1	1	1	1	1	1	1	1	1	
DMNH 82910	2	1	2	1	1	1	1	1	1	1	1	1	1	1	1	1	1	
DMNH 82944	2	1	2	1	1	1	1	1	1	1	1	1	1	1	1	1	1	
*DMNH 83058	2	1	2	1	1	1	1	1	1	1	1	1	0	1	1	1	1	
DMNH 83131	2	1	2	1	1	1	1	1	1	1	1	1	1	1	1	1	1	
DMNH 83585	0	0	0	0	0	0	0	0	0	1	0	0	0	0	0	0	0	
*DMNH 83586	0	0	0	0	1	0	0	0	0	1	0	0	0	0	0	0	0	
DMNH 83587	0	0	0	0	1	0	0	0	0	1	0	0	0	0	0	0	0	
*DMNH 83588	0	0	1	0	1	1	0	0	0	1	0	0	1	0	0	0	0	

APPENDIX 2 *Continued*

Specimen number	Character number																	
	1	2	3	4	5	6	7	8	9	10	11	12	13	14	15	16	17	18
*DMNH 83589	0	0	0	0	1	1	0	0	0	1	0	0	0	0	0	0	0	
*DMNH 83590	0	0	1	0	1	1	0	0	0	1	0	0	0	0	0	0	0	
DMNH 83591	2	1	2	1	1	1	1	1	1	1	1	1	1	1	1	1	1	
DMNH 83592	1	1	1	0	1	1	1	1	1	1	1	1	1	1	1	1	0	
Humerus																		
*Outgroup	0	0	0	0	0	0	0	0	0	0	0	0	0	0				
*DMNH 35657	2	1	2	1	1	1	1	1	1	1	1	1	1	1				
DMNH 73061	2	1	2	1	1	1	1	1	1	1	1	1	1	1				
DMNH 73095	2	1	2	1	1	1	1	1	1	1	1	1	1	1				
DMNH 76523	2	1	2	1	1	1	1	1	1	1	1	1	1	1				
DMNH 76661	2	1	2	1	1	1	1	1	1	1	1	1	1	1				
*DMNH 76826	1	1	1	1	1	1	1	1	1	1	1	0	1	?				
DMNH 76856	2	1	2	1	1	1	1	1	1	1	1	1	1	1				
*DMNH 76885	0	1	0	0	0	0	0	0	0	0	1	0	1	0				
DMNH 77001	2	1	2	1	1	1	1	1	1	1	1	1	1	1				
DMNH 77084	2	1	2	1	1	1	1	1	1	1	1	1	1	1				
DMNH 77107	2	1	2	1	1	1	1	1	1	1	1	1	1	1				
DMNH 77108	2	1	2	1	1	1	1	1	1	1	1	1	1	1				
DMNH 77170	2	1	2	1	1	1	1	1	1	1	1	1	1	1				
DMNH 77234	2	1	2	1	1	1	1	1	1	1	1	1	1	1				
DMNH 77256	2	1	2	1	1	1	1	1	1	1	1	1	1	1				
DMNH 77273	2	1	2	1	1	1	1	1	1	1	1	1	1	1				
DMNH 77287	2	1	2	1	1	1	1	1	1	1	1	1	1	1				
DMNH 77371	2	1	2	1	1	1	1	1	1	1	1	1	1	1				
DMNH 77472	2	1	2	1	1	1	1	1	1	1	1	1	1	1				
DMNH 77751	2	1	2	1	1	1	1	1	1	1	1	1	1	1				
DMNH 77767	2	1	2	1	1	1	1	1	1	1	1	1	1	1				
*DMNH 77823	2	1	2	1	1	1	1	1	1	1	1	1	1	0				
DMNH 78063	2	1	2	1	1	1	1	1	1	1	1	1	1	1				
DMNH 78064	2	1	2	1	1	1	1	1	1	1	1	1	1	1				
DMNH 78271	2	1	2	1	1	1	1	1	1	1	1	1	1	1				
DMNH 78408	2	1	2	1	1	1	1	1	1	1	1	1	1	1				
DMNH 78423	2	1	2	1	1	1	1	1	1	1	1	1	1	1				
*DMNH 78452	1	1	1	1	1	1	1	1	1	1	1	0	1	0				
DMNH 78500	2	1	2	1	1	1	1	1	1	1	1	1	1	1				
DMNH 78503	2	1	2	1	1	1	1	1	1	1	1	1	1	1				
*DMNH 78603	2	1	1	1	1	1	1	1	1	1	1	0	1	0				
DMNH 78628	2	1	2	1	1	1	1	1	1	1	1	1	1	1				
DMNH 78681	2	1	2	1	1	1	1	1	1	1	1	1	1	1				
DMNH 79329	2	1	2	1	1	1	1	1	1	1	1	1	1	1				
DMNH 79337	2	1	2	1	1	1	1	1	1	1	1	1	1	1				
DMNH 79340	2	1	2	1	1	1	1	1	1	1	1	1	1	1				
DMNH 79452	2	1	2	1	1	1	1	1	1	1	1	1	1	1				
DMNH 79989	2	1	2	1	1	1	1	1	1	1	1	1	1	1				
DMNH 80059	2	1	2	1	1	1	1	1	1	1	1	1	1	1				
DMNH 80060	2	1	2	1	1	1	1	1	1	1	1	1	1	1				
DMNH 80062	2	1	2	1	1	1	1	1	1	1	1	1	1	1				
DMNH 80066	2	1	2	1	1	1	1	1	1	1	1	1	1	1				
DMNH 80067	2	1	2	1	1	1	1	1	1	1	1	1	1	1				
DMNH 80068	2	1	2	1	1	1	1	1	1	1	1	1	1	1				
DMNH 80472	2	1	2	1	1	1	1	1	1	1	1	1	1	1				
DMNH 80844	2	1	2	1	1	1	1	1	1	1	1	1	1	1				

APPENDIX 2 *Continued*

Specimen number	Character number																	
	1	2	3	4	5	6	7	8	9	10	11	12	13	14	15	16	17	18
DMNH 80846	2	1	2	1	1	1	1	1	1	1	1	1	1	1				
DMNH 80847	2	1	2	1	1	1	1	1	1	1	1	1	1	1				
DMNH 80850	2	1	2	1	1	1	1	1	1	1	1	1	1	1				
DMNH 80851	2	1	2	1	1	1	1	1	1	1	1	1	1	1				
DMNH 81352	1	1	1	1	1	1	1	1	1	1	1	0	1	0				
*DMNH 81353	1	1	1	1	1	1	0	1	1	1	1	0	1	0				
DMNH 81354	2	1	2	1	1	1	1	1	1	1	1	1	1	0				
*DMNH 81978	0	1	0	0	0	0	0	0	0	0	0	0	0	0				
DMNH 81979	0	1	0	0	0	0	0	0	0	0	0	0	0	0				
*DMNH 82228	1	1	1	1	1	1	1	1	1	1	1	1	1	1				
*DMNH 82247	1	1	1	0	1	1	0	0	1	1	1	0	1	0				
DMNH 82270	2	1	2	1	1	1	1	1	1	1	1	1	1	1				
*DMNH 82271	1	1	1	1	1	1	1	1	1	1	1	0	1	1				
DMNH 82543	2	1	2	1	1	1	1	1	1	1	1	1	1	1				
DMNH 82688	0	1	0	0	0	0	0	0	0	0	0	0	0	0				
*DMNH 82727	0	1	0	0	1	0	0	0	0	0	0	0	1	0				
DMNH 82729	2	1	2	1	1	1	1	1	1	1	1	1	1	1				
DMNH 82730	2	1	2	1	1	1	1	1	1	1	1	1	1	1				
*DMNH 82731	2	1	1	1	1	1	1	1	1	1	1	1	1	0				
DMNH 82732	2	1	2	1	1	1	1	1	1	1	1	1	1	1				
DMNH 82766	2	1	2	1	1	1	1	1	1	1	1	1	1	1				
DMNH 82767	2	1	2	1	1	1	1	1	1	1	1	1	1	1				
DMNH 82910	2	1	2	1	1	1	1	1	1	1	1	1	1	1				
DMNH 82944	2	1	2	1	1	1	1	1	1	1	1	1	1	1				
DMNH 83058	2	1	2	1	1	1	1	1	1	1	1	1	1	1				
DMNH 83131	2	1	2	1	1	1	1	1	1	1	1	1	1	1				